1 **Cortical networks for encoding near and far space**

2 **in the non-human primate**

3

4

5 Justine Cléry, Olivier Guipponi, Soline Odouard, Claire Wardak, Suliann Ben Hamed

6

7 *Institut des Sciences Cognitives Marc Jeannerod, UMR5229, CNRS*-Université Claude

8 Bernard Lyon I*, 67 Boulevard Pinel, 69675 Bron, France*

9

10

11 **Corresponding author:** Suliann Ben Hamed, benhamed@isc.cnrs.fr

12 **Keywords:** near space, peripersonal space, far space, macaque monkey, fMRI.

13 **Running title:** Near and Far Space processing in the Non-Human Primate.

14

15

16    **Abstract**

17          While extra-personal space is often erroneously considered as a unique entity, early

18    neuropsychological studies report a dissociation between near and far space processing both

19    in humans and in monkeys. Here, we use functional MRI in a naturalistic 3D environment to

20    describe the non-human primate near and far space cortical networks. We describe the co-

21    occurrence of two extended functional networks respectively dedicated to near and far space

22    processing. Specifically, far space processing involves occipital, temporal, parietal, posterior

23    cingulate as well as orbitofrontal regions not activated by near space, possibly subserving the

24    processing of the shape and identity of objects. In contrast, near space processing involves

25    temporal, parietal and prefrontal regions not activated by far space, possibly subserving the

26    preparation of an arm/hand mediated action in this proximal space. Interestingly, this network

27    also involves somatosensory regions, suggesting a cross-modal anticipation of touch by a

28    nearby object. Last, we also describe cortical regions that process both far and near space with

29    a preference for one or the other. This suggests a continuous encoding of relative distance to

30    the body, in the form of a far-to-near gradient. We propose that these cortical gradients in

31    space representation subserve the physically delineable peripersonal spaces described in

32    numerous psychology and psychophysics studies.

33

34

35

3

36    **Highlights:**

37    • Near space processing involves temporal, parietal and prefrontal regions.

38    • Far space activates occipital, temporal, parietal, cingulate & orbitofrontal areas.

39    • Most regions process both far & near space, with a preference for one or the other.

40    • Far-to-near gradient may subserve behavioral changes in peripersonal space size.

41

42

43

44    **INTRODUCTION**

45    Our environment is often perceived as a unitary space, however growing evidence

46    demonstrates that the brain contains a modular and a dynamic representation of space. Early

47    neuropsychological reports demonstrate that the unilateral ablation of the frontal eye fields

48    produces, in monkeys, an inattention to contralateral objects, more pronounced for far than for

49    near objects (Rizzolatti et al., 1983). In contrast, the inattention to contralateral objects

50    produced by the unilateral ablation of premotor area 6 is more pronounced for near than for

51    far objects (Rizzolatti et al., 1983). In 1991, a single case study presents the first

52    neuropsychological evidence for a left neglect in near space but not in far space after a

53    unilateral right hemisphere stroke in humans (Halligan and Marshall, 1991). The finding of

54    the opposite dissociation confirms that, as for monkeys, far and near space are separately

55    coded by the human brain (Cowey et al., 1994, 1999; Vuilleumier et al., 1998), though a task

56    dependence of far and near space processing deficits is reported (Aimola et al., 2012; Keller et

57    al., 2005).

58    In recent years, fMRI studies show that the coding of near space involves a dorsal

59    network including the left dorsal occipital and intraparietal cortex and the left ventral

60    premotor cortex, while the coding of far space involves a ventral network including the

61    ventral occipital cortex bilaterally and the right medial temporal cortex (Aimola et al., 2012;

62    Weiss et al., 2000).

63    Peripersonal neurons fire both when a tactile stimulus is delivered to the animal's skin

64    and when a visual stimulus is presented in the space near the part of the body where the tactile

65    field is located. These have been described in several cortical regions: the prefrontal cortex

66    (Fogassi et al., 1996; Gentilucci et al., 1988; Graziano et al., 1994; Gross and Graziano,

67    1995); in the parietal cortex where Hyvärinen and Poranen (1974) describe the visual

68    response of parietal neurons "as an anticipatory activation" that appears before the neuron's

69    tactile RF is touched. The multimodal ventral intraparietal area VIP stands out in this respect

70    (Duhamel et al., 1998; Avillac et al., 2004, 2007, Guipponi et al., 2013, 2015a; Wardak et al.,

71    2016). This region encodes both large field visual movement mimicking the consequences of

72    the displacement of a subject within its environment (Bremmer et al., 2000, 2002a, 2002b)

73    and the movement of visual objects within the near peripersonal space (Bremmer et al., 1997,

74    2013). A first study did not identify a sensitivity to the 3-dimensional structure of static

75    stimuli in VIP (Durand et al., 2007), however a more recent study shows that VIP is involved

76    in depth-structure processing (Van Dromme et al., 2016). In comparison, human VIP shows

77    no preference for any particular spatial range (Quinlan and Culham, 2007).

78         Beyond these two prefrontal and parietal cortical regions, little is known about the

79    whole brain network that is involved in far and near space processing in monkeys. In

80    particular, while several functional magnetic resonance imaging (fMRI) studies describe the

81    cortical regions involved in the processing of 3-dimensional shape from disparity (Durand et

82    al., 2009; Joly et al., 2009) or shading and texture (Nelissen et al., 2009), to our knowledge,

83    no study to date provides, in this specie, a description of the cortical networks involved in the

84    processing of far and near space. fMRI performed in monkeys bridges the gap between human

85    fMRI and monkey invasive methodologies, and allows to identify and localize the activations

86    in specific voxels, beyond cytoarchitectonic definitions of functional areas to guide future

87    electrophysiological recordings. Here, we use fMRI in monkeys immersed in a naturalistic 3D

88    environment to describe a functional gradient going from selective near space coding, to

89    preferential near space coding, to unselective space coding, to preferential far space coding

90    and selective far space coding. We also describe a cortical network activated by intrusion into

91    peripersonal space. Interestingly, this network is only partially overlapping with the near

92    space coding network. Overall, these observations argue for multiple space representations the

93    functional significance of which remains to be assigned.

94    **MATERIAL AND METHODS**

95    All procedures were in compliance with the guidelines of European Community on

96    animal care (European Community Council, Directive No. 86–609, November 24, 1986). All

97    the protocols used in this experiment were approved by the animal care committee

98    (Department of Veterinary Services, Health & Protection of Animals, permit number 69 029

99    0401) and the Biology Department of the University Claude Bernard Lyon 1. The animals'

100   welfare and the steps taken to ameliorate suffering were in accordance with the

101   recommendations of the Weatherall report, "The use of non-human primates in research".

102

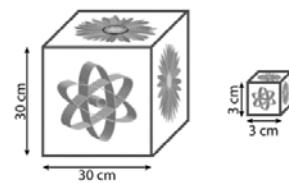103   *Subjects and experimental setup*

104   Two rhesus monkeys (female MZ, male MT, 10-8 years old, 6-10 kg) participated to

105   the study. The animals were implanted with a plastic MRI compatible headset covered by

106   dental acrylic. The anesthesia during surgery was induced by Zoletil (Tiletamine-Zolazepam,

107   Virbac, 15 mg/kg) and followed by Isoflurane (Belamont, 1-2%). Post-surgery analgesia was

108   ensured thanks to Temgesic (buprenorphine, 0.3 mg/ml, 0.01 mg/kg). During recovery, proper

109   analgesic and antibiotic coverage were provided. The surgical procedures conformed to

110   European and National Health guidelines for the care and use of laboratory animals.

111   During the scanning sessions, monkeys sat in a sphinx position in a plastic monkey

112   chair positioned within a horizontal magnet (1.5-T MR scanner Sonata; Siemens, Erlangen,

113   Germany). Their head was restrained and they were equipped with MRI-compatible

114   headphones customized for monkeys (MR Confon GmbH, Magdeburg, Germany). A radial

115   receive-only surface coil (10-cm diameter) was positioned above the head. Monkeys were

116   required to fixate a LED placed at 90 cm away from their face, at eye level, aligned with their

117   sagittal axis. Eye position was monitored at 120 Hz during scanning using a pupil-corneal

118   reflection tracking system (Iscan®, Cambridge, MA). The calibration procedure involved the
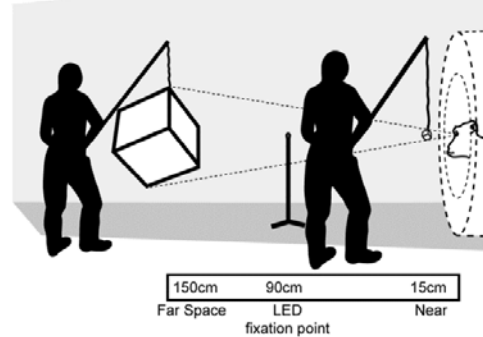
119    fixation LED and 4 additional LEDs, placed in the same coronal plane as the fixation LED.

120    All five LEDs were sequentially switched on and off and the monkey was rewarded for

121    orienting and maintaining its gaze towards the illuminated LED. These four additional LEDs

122    were subsequently removed during the main task during which only the central LED was

123    present. Monkeys were rewarded with liquid dispensed by a computer-controlled reward

124    delivery system (Crist®) thanks to a plastic tube coming to their mouth. The reward

125    probability and quantity increased as fixation duration increased according to a subject-

126    specific schedule, thus positively reinforcing fixation behavior. Fixation was considered as

127    successful when the eyes remained in a window of 1.5° around the fixation LED. The reward

128    schedule was uncorrelated with the scanning schedule. The task and all the behavioral

129    parameters were controlled by two computers running Matlab® and Presentation®. Monkeys

130    were trained in a mock scan environment approaching to the best the actual MRI scanner

131    setup. Actual scanning was performed once their fixation performance was maximized (>85-

132    90% of time inside the tolerance window).

133    **Figure 1:** Experimental fMRI protocol. A) 3D naturalistic stimuli, a large 30x30x30

134    cm3 cube and an identical small 3x3x3 cm3 cube. The 6 faces of each transparent cube

135    were decorated with 6 different fractal images. B) Block design. C) Experimental set

136    up. Near space (15 cm from the monkey's face) and far space (150 cm from the

137    monkey's face) were stimulated with the two types of 3D stimuli (same apparent

138    sizes). Fixation is achieved at an intermediate position (red fixation LED, at 90cm). D)

139    Summary of contrast analyses performed to extract the networks of interest: condition

140    of interest higher than fixation (first column), preferential coding of condition of

141    interest (second column) and selective coding of condition of interest (third column).
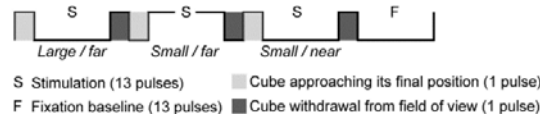
142

## A) Stimuli

## B) Blocked fMRI design

## C) Experimental setup

## D) Summary of the contrast analyses



| Small Near space | Preferential Near space | Selective Near space |
|---|---|---|
| Small Near >> Fixation | Small Near >> Big Far **AND** Small Near >> Fixation *(inclusive mask)* (1) | Small Near >> Big Far **AND** Small Near >> Fixation *(inclusive mask)* **AND** **NOT** Big Far >> Fixation *(exclusive mask)* (2) |
| Big Far space | Preferential Far space | Selective Far space |
| Big Far >> Fixation | Big Far >> Small Near **AND** Big Far >> Fixation *(inclusive mask)* (3) | Big Far >> Small Near **AND** Big Far >> Fixation *(inclusive mask)* **AND** **NOT** Small Near >> Fixation *(exclusive mask)* (4) |
| Small Far space | Preferential Object size | Selective Object size |
| Small Far >> Fixation | Big Far >> Small Far **AND** Big Far >> Fixation *(inclusive mask)* (4) | Big Far >> Small Far **AND** Big Far >> Fixation *(inclusive mask)* **AND** **NOT** Small Far >> Fixation *(exclusive mask)* (6) |
| Looming Near object | Preferential Looming | Selective Looming |
| Looming >> Fixation | Looming >> Small Near **AND** Looming >> Fixation *(inclusive mask)* (5) | Looming >> Small Near **AND** Looming>> Fixation *(inclusive mask)* **AND** **NOT** Small Near >> Fixation *(exclusive mask)* (8) |

143

## *Task and stimuli*

145    The animals were trained to maintain fixation on the central LED. This allowed to

146    control for eye vergence signals all throughout the experimental runs. An enriched stable

147    visual scene was installed around the fMRI aperture, in front of the monkeys, so as to

148      maximize depth cues (2m high lateral black curtains hiding the experimenters, large wooden

149      static sticks placed along the curtains and in the back of the room, visible to the monkeys

150      throughout the experiment). Once this behavior was stabilized, monkeys were further trained

151      to maintain fixation while 3D objects were presented at either an average of 15 cm in front of

152      their eyes (i.e. in the space between their head and the fixation LED, see Figure 1C) or at an

153      average of 150 cm (i.e. in the space beyond the fixation LED, see Figure 1C), thus allowing to

154      stimulate the space situated respectively near and far from the animals. Stimulations were

155      achieved with either a small cube (3x3x3 cm) or a large cube (30x30x30 cm, Figure 1A),

156      attached to a rigid holding stick. These cubes had the same apparent size when the small cube

157      was placed at 15cm from the subject and the larger cube was placed at 150cm (Figure 1C),

158      thus allowing to control for size effects. These cubes were constructed with transparent plastic

159      material and the presentation of the near small object did not hide the fixation LED from the

160      monkey. In order to maximize depth cues, the edges of the cubes were highlighted with red

161      stripes and their transparent faces were ornamented with fractal pictures, resized for each cube

162      such that the edges and the images occupied the same proportion in each cube (Figure 1A).

163      Each cube was attached to a thin wooden stick by means of a transparent nylon cord. During

164      the stimulation duration, the cube was continuously agitated by the experimenter so as to

165      prevent neuronal habituation, but only the cube and the stick were visible to the monkeys, as

166      the experimenters stayed hidden behind the curtains. To confine visual stimulation to a depth

167      range, marks were placed on the floor, on the sticks holding the cubes as well as on the

168      curtains hiding the experimenter. Experimenter manipulating the large cube controlled the

169      manipulation of the small cube by the other experimenter and vice versa. Experimenters

170      flipped from large cube to small cube manipulation from one scanning session to the other, so

171      as to minimize experimental systematic biases. In this context, and given the size of the cubes

172      and the fact that these were agitated in all directions, the localization error of the cubes can be

173    considered as marginal. Three conditions were tested in blocks of 13 pulses: 1) the small cube

174    presented in the near space; 2) the small cube presented in the far space and 3) the big cube

175    presented in the far space. Both during training and testing, the cubes were approached (1

176    pulse), agitated (13 pulses) and withdrawn (1 pulse) from the target location (near or far

177    space) by two experimenters out of the field of view (behind the black opaque curtains), one

178    controlling the small cube and the other the large cube. The stimulation instructions (count

179    down, type of stimulation, pulse counts etc.) were delivered to them on a computer screen

180    placed next to them and coupled to the experimental control system.

181         Functional time series (runs) were organized as follows (Figure 1B): a 13-volume

182    block of stimulation category 1 was followed by a 13-volume block of stimulation category 2,

183    a 13-volume block of stimulation category 3, and a 13-volume block of pure fixation

184    (baseline). Before the beginning (resp. after the end) of each block of stimulation, 1 pulse was

185    dedicated to the approach (resp. withdrawal) of the appropriate cube towards (resp. away

186    from) the target space. Approaching or withdrawing the cubes involved only a minimal

187    displacement of the curtains, thanks to two vertical slits in the curtains, placed respectively

188    close to the magnet bore or at 150cm from the monkey. These slits were firmly closed back

189    during the main stimulation blocks. A given sequence was played three times, resulting in a

190    174-volume run. The blocks for the 3 categories were presented in 6 counterbalanced possible

191    orders.

192         A previous study involving both these monkeys (Guipponi et al., 2015a) and using a

193    classical retinotopy localizer (Fize et al., 2003), allowed us to generate individual whole brain

194    maps of center vs. periphery visual coding (see Supplementary data S1).

195

196    ***Scanning***

197     Before each scanning session, a contrast agent, monocrystalline iron oxide

198     nanoparticle (Feraheme®, Vanduffel et al., 2001), was injected into the animal's

199     femoral/saphenous vein (4-10 mg/kg). Brain activations produce increased BOLD signal

200     changes. In contrast, when using MION contrast agents, brain activations produce decreased

201     signal changes (Kolster et al., 2014). For the sake of clarity, the polarity of the contrast agent

202     MR signal changes, which corresponds essentially to a cerebral blood volume (CBV)

203     measurement, was inverted. We acquired gradient-echo echoplanar (EPI) images covering the

204     whole brain (1.5 T; repetition time (TR) 2.08 s; echo time (TE) 27 ms; 32 sagittal slices;

205     2x2x2-mm voxels). A total of 34 (22) runs was acquired for MZ (/MT).

206

207     ***Analysis***

208     A total of 20 (15) runs were selected based on the quality of the monkeys' fixation

209     throughout each run (>80% within the tolerance window). Time series were analyzed using

210     SPM8 (Wellcome Department of Cognitive Neurology, London, United Kingdom). For

211     spatial preprocessing, functional volumes were first realigned and rigidly coregistered with

212     the anatomy of each individual monkey (T1-weighted MPRAGE 3D 0.6x0.6x0.6 mm or

213     0.5x0.5x0.5 mm voxel acquired at 1.5T) in stereotactic space. The JIP program (Mandeville et

214     al., 2011) was used to perform a non-rigid coregistration (warping) of a mean functional

215     image onto the individual anatomies.

216     Fixed effect individual analyses were performed for each condition in each monkey,

217     with a level of significance set at $p<0.05$ corrected for multiple comparisons (FWE, $t>4.8$,

218     unless stated otherwise).

219     To define the ***preferential near space network***, we contrasted the cortical activations

220     obtained by the stimulation of near space by a small object to those obtained by the

221     stimulation of far space by a large object of the same apparent size as the small object in the

222    near space and was additionally masked by the activations obtained by the stimulation of near

223    space by a small object contrasted by fixation condition (inclusive 'near space stimulation vs.

224    fixation' mask, p=0.05 corrected for multiple comparisons, FWE, see Figure 1D, (1)). To

225    define the *selective near space network*, the above preferential near space network was

226    additionally masked by the activations obtained by far space stimulations (exclusive 'far

227    space stimulation vs. fixation' mask, p=0.05 corrected for multiple comparisons, FWE, see

228    Figure 1D, (2)). To define the *preferential far space network*, we contrasted the cortical

229    activations obtained by the stimulation of far space by a large object of the same apparent size

230    as the small object in the near space to those obtained by the stimulation of near space by a

231    small object and was additionally masked by the activations obtained by the stimulation of far

232    space by a large object contrasted by fixation condition (inclusive 'far space stimulation vs.

233    fixation' mask, p=0.05 corrected for multiple comparisons, FWE, see Figure 1D, (3)). To

234    define the *selective far space network*, the above preferential far space network was

235    additionally masked by the activations obtained by near space stimulations (exclusive 'near

236    space stimulation vs. fixation' mask, p=0.05 corrected for multiple comparisons, FWE, see

237    Figure 1D, (4)).

238        To define the *preferential encoding of the large cube in the far space network*, we

239    contrasted the cortical activations obtained by the stimulation of far space by a large object to

240    those obtained by the stimulation of far space by a small object and was additionally masked

241    by the activations obtained by the stimulation of far space by a large object contrasted by

242    fixation condition (inclusive 'Large far space stimulation vs. fixation' mask, p=0.05 corrected

243    for multiple comparisons, FWE, see Figure 1D, (5)). To define the *selective encoding of the*

244    *large cube in the far space network*, the above preferential encoding of the large cube in the

245    far space network was additionally masked by the activations obtained by the stimulation of

246    far space by a small object (exclusive 'Small far space stimulation vs. fixation' mask, p=0.05

247  corrected for multiple comparisons, FWE, see Figure 1D, (6)). To define the **specific looming**

248  **toward near space network**, we contrasted the cortical activations obtained by the looming of

249  a small object toward near space to those obtained by the stimulation of near space by a small

250  object and was additionally masked by the activations obtained by the looming of a small

251  object toward near space contrasted by fixation condition (inclusive 'looming toward near

252  space vs. fixation' mask, p=0.05 corrected for multiple comparisons, FWE, Figure 1D, (7))

253  and masked by the activations obtained by near space stimulations (exclusive 'near space

254  stimulation vs. fixation' mask, p=0.05 corrected for multiple comparisons, FWE, Figure 1D,

255  (8)).

256       In all analyses, realignment parameters, as well as eye movement traces, were included

257  as covariates of no interest to remove eye movement and brain motion artifacts. When

258  coordinates are provided, they are expressed with respect to the anterior commissure. Results

259  are displayed on flattened maps obtained with Caret, for each monkey (Van Essen et al. 2001;

260  http://www.nitrc.org/projects/caret/). The results were consistent in the two animals for all the

261  discussed cortical regions (i.e. activations observed in at least 3 out of 4 hemispheres) and do

262  not reveal blink (Guipponi et al., 2015b) or saccade-related activations (see results). Thus,

263  figures 6, 7 and 8 correspond to a group analysis, so as to simplify the presentation of the

264  results. In this case, fixed effect group analyses were performed for each sensory modality

265  and for conjunction analyses with a level of significance set at p<0.05 corrected for multiple

266  comparisons (FWE, t>4.8) and projected onto the anatomy of monkey MT. In order to have

267  an unbiased group analysis, we selected the 15 best runs of MZ (in term of fixation

268  performance), so as to have the same number of runs for each monkey. The results are then

269  displayed on the flattened and fiducial maps of MT.

270       Assigning the activations to a specific cortical area was performed on each individual

271  monkey       brain       using       the       monkey       brain       atlases       made       available       on

272    http://scalablebrainatlas.incf.org. These atlases allow mapping specific anatomical coronal

273    sections with several cytoarchitetonic parcellation studies. We used the Lewis and Van Essen

274    (2000) and the Paxinos Rhesus Monkey (2000) atlases.

275        *Regions of interest.* We performed regions of interest (ROI) analyses using MarsBar

276    toolbox (Brett et al., 2002), based on the fixed effects individual analyses results. We defined

277    geometric cubic ROIs (2x2x2 mm) centered on the local maximum t-score based on one of

278    the activations obtained for each contrast at FWE-corrected level (*t*-scores>4.8). This ROI

279    analysis only serves to illustrate how PSC changed, within each functional network, as a

280    function of the type of visual stimulation: the specific near space activations, the preference

281    near activations, the unselective near-far space activations, the preference far activations and

282    the specific far space activations. It is thus fully redundant with the flat map analysis. The

283    percent of signal change (PSC) are extracted for each ROI for all the runs using SPM8 and the

284    MarsBar toolbox. The significance of these PSCs across all runs was assessed using a one-

285    tailed paired t-test, in Matlab™ (The MathWorks Inc., Natick, MA, USA).

286        *Eye movements data analysis.* During the MRI scanning sessions, the horizontal (X)

287    and vertical (Y) eye position of the monkey was recorded (in degree) from one eye. An

288    example of the time course of eye position is presented in Figure 2A and 2B, for an exemplar

289    run. For each of these exemplar runs, the block structure is indicated. The refined analysis of

290    eye movements on all the runs per monkey demonstrates that, on average, the monkeys

291    succeeded in maintaining their eyes within the fixation window all throughout the run,

292    irrespective of the type of sensory manipulation (Friedman test >0.05, data not shown). The

293    average and standard deviation of microsaccade and saccade duration with respect to the total

294    blocks duration over all sessions are shown in Figure 2C. These differ as a function of

295    stimulation block (Kruskall-wallis: p<0.001 for MZ and p<0.01 for MT). In supplementary

296    figure S2, a precise description of the expected range of eye movements for each type of

14

297     stimuli if the monkeys had been fixation and tracking the stimulation objects rather than

298     maintaining vergence onto the fixation spot is provided. This analysis shows that any tracking

299     of the object would have resulted in a significant increase in out of the fixation window
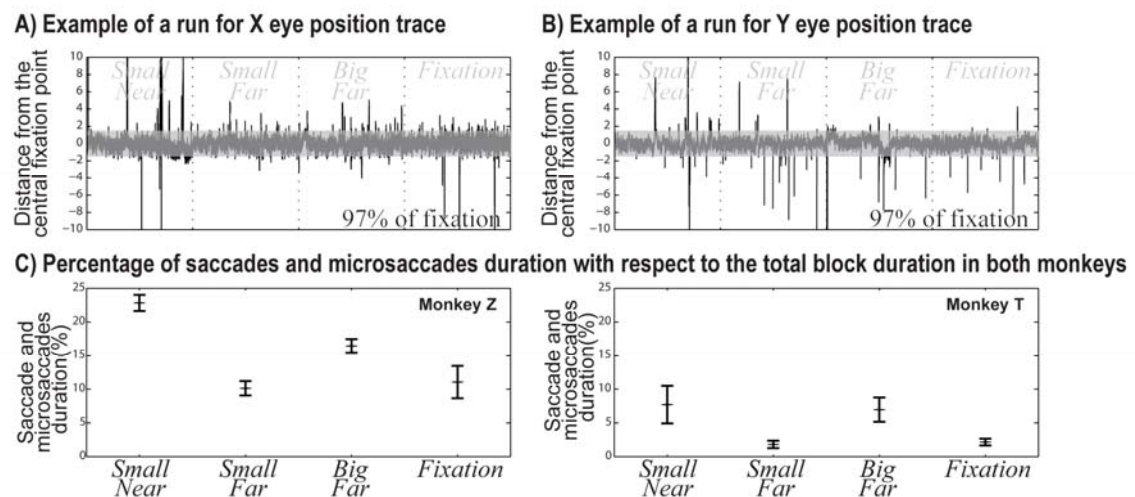
300     epochs, beyond what is observed experimentally.



301

302     **Figure 2:** Analysis of eye movements as function of stimulation blocks. 2A) X and

303     2B) Y eye traces for an exemplar run. 2C) Average and standard deviation of

304     microsaccade and saccade duration with respect to the total blocks duration over all

305     sessions (Kruskall-wallis: $p<0.001$ for MZ and $p<0.01$ for MT).

306

307     ***Signal to noise ratio (SNR).*** We calculated the temporal SNR for both monkeys to

308     check for inhomogeneities between the two hemispheres of each animal. The signal is quite

309     homogeneous on the maps (see Supplementary data S3). The apparent asymmetry between

310     the activation strengths on the different contrasts are most probably to the fact that the

311     experimenters were always located on the left side of the monkey, hence the higher right

312     cortical activations.

313    **RESULTS**

314    Monkeys were exposed, in the same time series, to naturalistic near or far space

315    stimulations (Figure 1), while maintaining their gaze at an intermediate fixation location, so as

316    to keep vergence signals constant all throughout the recording runs. This design allows us to

317    describe the cortical networks involved in near and far space processing in naturalistic

318    conditions. The reported activations in figures 3, 4 and 5 are identified using an individual

319    analysis, with a level of significance set at $p<0.05$, corrected for multiple comparisons (FWE,

320    $t>4.8$). The reported activations in figures 6, 7 and 8 are identified using a group analysis,

321    with a level of significance set at $p<0.05$, corrected for multiple comparisons (FWE, $t>4.8$).

322    As a result, they reflect the activations that are common to the two monkeys involved in the

323    study.

324

325    *Interaction of naturalistic presentations with saccadic behavior*

326    The monkeys are required to fixate a fixation led placed at 90 cm from their face, while being

327    presented with either a small (3cm) cube very close to the face or a large (30cm) cube in the

328    far space. An important question is to characterize the effect of these stimuli onto saccadic

329    behavior and to check whether the monkeys were indeed maintaining vergence onto the

330    fixation led. A detailed analysis of the cumulated microsaccades and saccades duration are

331    shown in Figure 2C. These durations are significantly different following the block

332    stimulation in both monkeys (Kruskall-wallis: $p<0.001$ for MZ and $p<0.01$ for MT). Indeed,

333    the percentage of correct fixation changes following the block stimulation: 77.2% (/92.3%)

334    when the small cube stimulated the near space; 89.9% (98.2%) when the small cube

335    stimulated the far space; 83.6% (/93.0%) when the big cub stimulated the far space and 89.0%

336    (97.83%) during fixation only, for monkey Z (/monkey T respectively). In other words,

337    maintaining fixation during the near space stimulation by the small cube was the most

16

338    challenging. Were the monkeys tracking the near cube? Given the volume of near space that

339    was being explored by the small cube stimulation (Supplementary figure S2, upper row), if

340    the monkey had been tracking the object continuously, the out of the window eye epochs in

341    this condition would have been much larger than in the other conditions. This is an indirect

342    indication that the monkeys did try and suppress eye tracking of the near object during this

343    condition. Nonetheless, could this small systematic behavioral bias affect our functional

344    description of near specific activations? Anticipating on the core of the present work, no

345    specific frontal eye field area or lateral intraparietal area activations are observed during this

346    near space stimulation as compared to the far space stimulation. These two cortical regions

347    are involved in saccadic behavior and their activation is observed during saccadic behavior

348    (Everling and Munoz, 2000; Hutchison et al., 2012; Koyama et al., 2004; see for review

349    Womelsdorf and Everling, 2015).

350

351    **Naturalistic near and far space stimulations**

352    Naturalistic near space stimulations with a small cube (Figure 3, yellow upper maps,

353    small near vs. fixation contrast) activated a small extent of the occipital striate and extrastriate

354    areas, the temporal cortex (superior temporal sulcus), the parietal cortex, the prefrontal cortex

355    (arcuate sulcus and posterior and anterior parts of principal sulcus) as well as the orbitofrontal

356    cortex. Far space stimulations with a far cube with the same apparent size as the near small

357    cube (Figure 3, blue middle maps, big far vs. fixation contrast) also activated a widespread

358    cortical network including the entire striate and extrastriate cortex, the temporal cortex, the

359    parietal cortex, small portions of the prefrontal cortex along the arcuate sulcus as well as the

360    orbitofrontal cortex. When far space was stimulated using a cube of the same real size as the

361    small cube used for the near space stimulation (Figure 3, green lower maps, small far vs.

362    fixation contrast), a similar though smaller cortical network was activated. In the following,

363    we identify those cortical regions that are either preferentially or specifically involved in near

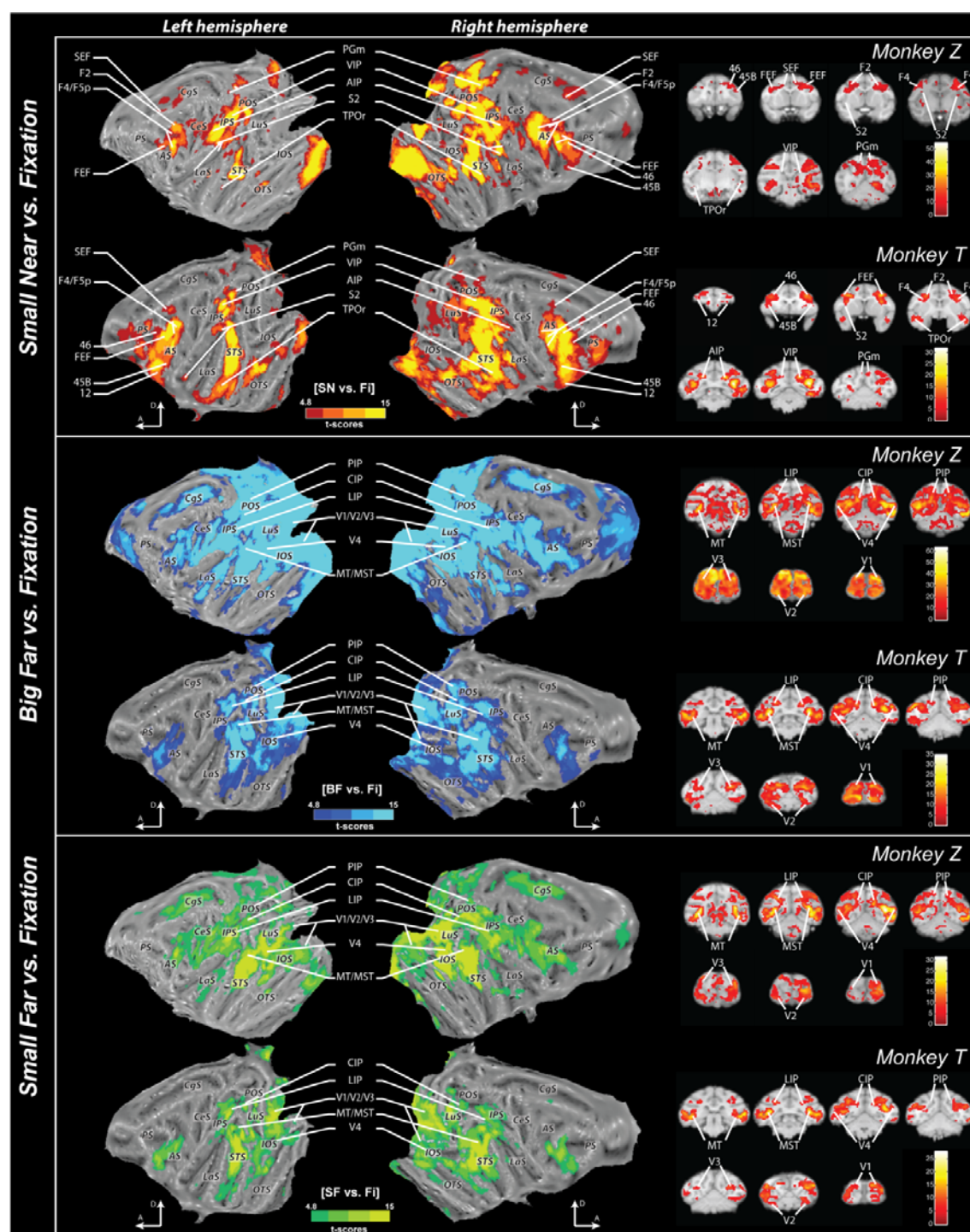364    space and far space processing respectively.



**Figure 3:** Near space and far space individual analyses. Activations are presented on

the flattened representation of the two monkey right and left hemispheres obtained

368       with Caret. The upper part of the figure shows the near space stimulated with the small

369       cube (SN) versus fixation contrast (t scores = 4.8 at $p<0.05$, FWE-corrected level in

370       the red scale). Middle and lower panels present the far space respectively stimulated

371       with the big (BF) and the small cubes (SF; t scores = 4.8 at $p<0.05$, FWE-corrected

372       level respectively in the blue and green scales). The right panel represents selected

373       coronal slices showing the activated areas for each contrast in both monkeys. A,

374       Anterior; D, Dorsal; SN: small near; BF: big far; SF: small far. 12, area 12; 45B, area

375       45B; 46, area 46; AIP, anterior intraparietal area AIP; CIP caudial intraparietal area;

376       F2, premotor area F2; FEF, frontal eye field; LIP, lateral intraparietal area LIP;

377       MT/MST, medial/superior temporal areas MT/MST; F4/F5, premotor areas F4/F5;

378       PGm, medial parietal area PGm; PIP, posterior intraparietal area PIP, S2,

379       somatosensory area 2; SEF: supplementary eye field; TPOr, rostral temporoparietal

380       occipital area TPOr; VIP, ventral intraparietal area VIP; V1/V2/V3/V4, visual areas

381       V1,V2,V3 or V4. Cortical sulci: AS, arcuate sulcus; CgS, cingulate sulcus; CeS,

382       central sulcus; IOS, inferior occipital sulcus; IPS, intraparietal sulcus; LaS, lateral

383       (Sylvian) sulcus; LuS, lunate sulcus; OTS, occipital temporal sulcus; POS, parieto-

384       occipital sulcus; PS, principal sulcus; STS, superior temporal sulcus.

385

386       In this Figure 3, the near space stimulation vs. fixation activation maps contrasts with

387    the far space stimulation vs. fixation activations maps in that central striate and extra-striate

388    cortex is spared in the former condition. While this can seem extremely surprising (as strong

389    central visual stimulation is expected to reliably activate these regions), this observation that

390    is reproduced in both monkeys corresponds to what one would expect if the monkeys were

391    fixating the fixation led and suppressing visual information away from the fixation plane.

392    Indeed, if one assumes an eye-to-eye distance of 2.6 cm, fixation vergence angle would be

393    around 1.65° and near cube stimulation would correspond to crossed visual binocular

394    disparities of 8°. V1 neurons are reported to be selective for absolute binocular disparities

395    below 1°, thus possibly accounting for our observations in this respect.

396

397    **Distinctions within the near space cortical network**

398         In the following, we define three different functional near space networks: a restricted

399    network selectively encoding near space; a larger network preferentially encoding near space

400    with respect to far space and an even larger network encoding near space irrespectively of any

401    coding for far space. The larger ***non-selective near space network*** corresponds to the one

402    identified in Figure 3 (yellow upper maps, represented in the Figure 4 as a red contour) and

403    discussed in the previous section. The ***preferential near space network*** (Figure 1D (1), Figure

404    4 A and C, dark red, Figure 8, dark red), activates bilateral cortical regions the contribution of

405    which is statistically higher for near space than for far space. These include parietal areas: the

406    posterior intraparietal sulcus (IPS: ventral intraparietal area VIP, the posterior medial

407    intraparietal area MIP) as well as its anterior most tip (possibly anterior intraparietal area

408    AIP), the medial parietal cortex (area PGm) and the parietal opercular region area 7op;

409    temporal areas: the rostral temporoparietal occipital area TPOr in the medial mid-to-anterior

410    bank of the superior temporal sulcus, the intraparietal sulcus associated area IPa, the inferior

411    temporal area TEAa-m, the dorsal portion of the subdivision TE1-3; insular regions:  the

412    parainsular cortex PI; somatosensory area SII within the medial bank of the lateral sulcus;

413    prefrontal and premotor regions: dorsal premotor cortex F2, premotor area 4C or F4/F5

414    including premotor zone PMZ, the supplementary eye field, the frontal eye fields (area 8a as

415    well as 8ac), prefrontal area 46p, prefrontal area 45B; frontal regions: the posterior

416    orbitofrontal area 12.

417    The *selective near space network* (Figure 1D (2), Figure 4 B and D, red to yellow color scale,

418    Figure 8, colored to yellow color scale, *t* scores = 4.8 and above, FWE-corrected level),

419    exclusively involved in near space processing activates discrete bilateral regions within the

420    majority of the cortical areas highlighted by the previous contrast.



421

422    **Figure 4:** Non-selective, preferential and specific near space networks. Activations are

423    presented on the flattened maps of individual monkeys. Only the key activations

21

424 identified in three hemispheres out of four are labelled. A and C) Non-selective and

425 preferential near space encoding for monkey Z (A) and T (C). Preferential near space

426 coding corresponds to the cortical regions whose activations are higher for the small

427 cube in near space than for the large cube in far space (t scores = 4.8 at p<0.05, FWE-

428 corrected level in the dark red). B and D) Non-selective and specific near space

429 encoding for monkey Z (B) and T (D). Specific near space encoding corresponds to

430 the cortical regions which are activated by the small near cube but not for the large far

431 cube (red to yellow scale, exclusive mask for far space versus fixation baseline applied

432 at FWE-corrected level p<0.05). The outer red contours correspond to non-selective

433 near space encoding (near space versus fixation, as in figure 3). For other conventions,

434 see Figure 3.

435

436 **Distinctions within the far space cortical network**

437 Likewise, we define three different functional far space networks: a restricted network

438 selectively encoding far space; a larger network preferentially encoding far space with respect

439 to near space and an even larger network encoding far space irrespectively of any coding for

440 near space. The larger ***non-selective far space network*** corresponds to the one identified in

441 Figure 3 (blue middle maps, represented in the Figure 5 as a blue contour) and discussed

442 above. The ***preferential far space network*** (Figure 1D (3), Figure 5 A and B: dark blue,

443 Figure 8, dark blue), activates bilateral cortical regions the contribution of which is

444 statistically higher for far space than for near space. A strong inter-individual variability can

445 be observed, these activations being larger in Monkey Z than in Monkey T. Differences in

446 global activation strength are often observed when performing single subject fMRI analyses.

447 In the present context, an alternative hypothesis can be put forward. Monkey Z is a small

448 female while monkey T is a large dominant male. The larger activations observed in monkey

22

449    Z could indicate higher overall activations to the presented naturalistic stimuli because of their

450    higher relative size with respect to body size, as compared to monkey T. This would need to

451    be confirmed experimentally. In the following, only the common activations are described.

452    These encompass the entire visual striate and extrastriate cortex: areas V1, V2, V3, V3A and

453    V4; they also include parietal cortical regions: the posterior intraparietal area PIP, the lateral

454    intraparietal area LIP, the medial parietal convexity (area 5v), the lateral parietal convexity

455    (area 7a, 7ab and 7b), as well as the posterior most part of the intraparietal sulcus (caudial

456    intraparietal area CIP, parietal reach region, PRR), these activities extending towards the

457    parieto-occipital cortex (including areas V6A and V6); temporal cortex: medial and superior

458    temporal area MT and MST.

459    When this contrast is additionally masked by the activations obtained by near space

460    stimulations, thus defining the *selective far space network*, a network that is selectively

461    involved in far space processing can be identified (Figure 1D (4), Figure 5 C and D, dark blue

462    to light blue color scale, Figure 8: dark blue to light blue color scale, *t* scores = 4.8 and above,

463    FWE-corrected level). This analysis describes discrete bilateral regions essentially in occipital

464    and temporal areas highlighted by the previous contrast and few parietal areas.

465        **Figure 5:** Non-selective, preferential and specific far space networks. Activations are

466        presented on the flattened maps of individual monkeys. Only the key activations

467        identified in three hemispheres out of four are labelled. A and C) Non-selective and

468        preferential far space encoding for monkey Z (A) and T (C). Preferential far space

469        coding corresponds to the cortical regions whose activations are higher for the large

470        cube in far space than for the small cube in near space (t scores = 4.8 at p<0.05, FWE-

471        corrected level in the dark blue). B and D) Non-selective and specific far space

472        encoding for monkey Z (B) and T (D). Specific far space encoding corresponds to the

473        cortical regions which are activated by the large far cube but not for the small near

23

474      cube (dark blue to light blue color scale, exclusive mask for near space versus fixation

475      baseline applied at FWE-corrected level p<0.05). The outer blue contours correspond

476      to non-selective far space encoding (far space versus fixation, as in figure 2). For other

477      conventions, see Figure 3.



478

479

480
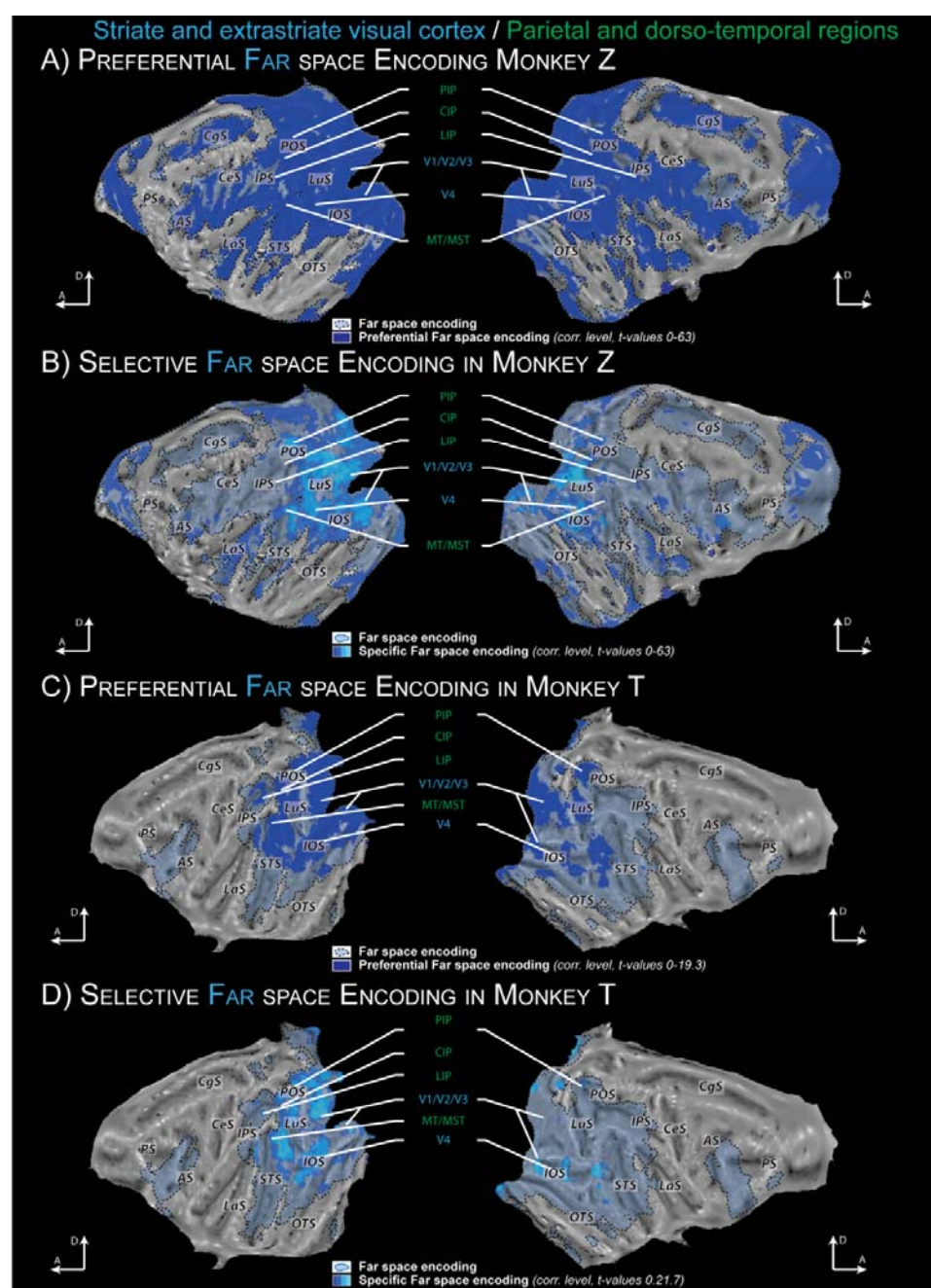
**Far space cortical network modulation by object size**

482     While the small cube presented in near space had the same apparent size as the far

483     cube presented in far space, these two objects had very different physical sizes ($3x3x3cm^3$

484     versus $30x30x30cm^3$). As a result, part of the far or near space network specificities described

485     above could have been due to this objective size difference (as opposed to an apparent size

486     difference). In order to address this issue, we now compare the cortical activations obtained

487     when stimulating far space with either a small cube or a large cube. For the sake of space, a

488     group analysis is performed rather than a single subject analysis. This group analysis captures

489     the common activations already described at the single individual level in figures 3, 4 and 5.

490     No activations are observed with the *small object in far space* versus *large object in far space*

491     contrast, indicating that all the cortical regions that are involved in processing the small object

492     in far space also contribute to the processing of the large object in far space. The inverse

493     contrast reveals a large cortical network (Figure 1D (5), Figure 6, dark blue) mostly identical

494     to that revealed by the *large cube in far space* versus *fixation* contrast (Figure 3, middle blue

495     panels). The network that is selective to the large cube in far space processing as compared to

496     the processing of smaller objects in far space (Figure 1D (6), Figure 6, dark blue to light blue

497     color scale, *t* scores = 4.8 and above, FWE-corrected level) includes large sectors of the visual

498     striate and extrastriate cortex, mostly coinciding with the peripheral visual field representation

499     (see Figure 4 in Guipponi et al., 2015 for an identification of these representations on this

500     same group of subjects), the parieto-occipital cortex, the posterior parietal cortex, the right

501     medial parietal cortex the anterior part of the superior temporal sulcus as well as a large extent

502     of the prefrontal cortex, the cingulate cortex, the orbitofrontal cortex and the frontal pole.
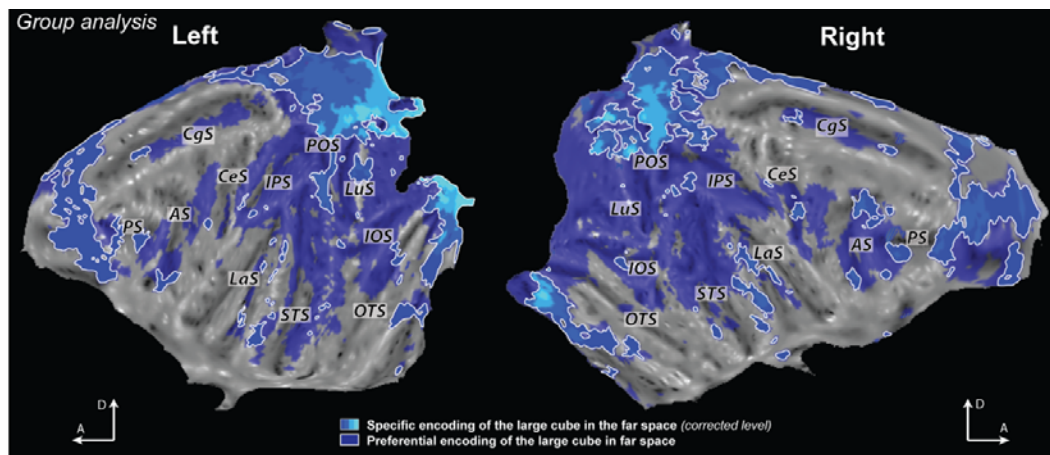
503

**Figure 6:** Preferential and specific encoding of the large cube in the far space. Activations are presented on the flattened maps of the reference monkey cortex (group analysis). Preferential encoding of the large cube in the far space corresponds to the cortical regions whose activations are higher for the big cube in far space than for the small cube in far space (t scores = 4.8 at p<0.05, FWE-corrected level in the dark blue). Specific encoding of the large cube in the far space corresponds to the cortical regions which are activated by the big cube but not for the small far cube in the far space (dark blue to light blue color scale, exclusive mask for the big cube in far space versus fixation baseline applied at FWE-corrected level p<0.05). For other conventions, see Figure 3.

**Figure 7:** Looming stimuli activate both Near and Far space network. Activations are presented on the flattened maps of the reference monkey cortex (group analysis). A, C and E, this presents the approach of the stimulus respectively towards near space with the small cube, towards far space with the small cube or towards far space with the big

27

519     cube versus fixation contrast (t scores = 4.8 at p<0.05, FWE-corrected level

520     respectively in the red, green and blue scale). B, D and F, this presents the receding of

521     the stimulus respectively from near space with the small cube, from far space with the

522     small cube or from far space with the big cube versus fixation contrast (t scores = 4.8

523     at p<0.05, FWE-corrected level respectively in the red, green and blue scale). On the

524     first panel (the approach of the stimulus towards near space with the small cube), the

525     black contours represent the near space encoding (one identified in Figure 3) and the

526     white contours represent the specific encoding of the approach of the small cube in the

527     near space which corresponds to the cortical regions which are activated by the

528     approach of the small cube in the near space but not by the near space encoding

529     (exclusive mask for the near space versus fixation baseline applied at FWE-corrected

530     level p<0.05). For other conventions, see Figure 3.

531

532     **Functional activations in response to looming and recession in near and far space.**

533     The physical approach of the cubes into far or near space and their recession back

534     behind the curtains was controlled by the experimenters following a precise schedule

535     indicated to them on a computer screen. The onsets of these displacements were logged

536     together with all other task events. Here, we focus on the activations observed during these

537     dynamic phases of the task (Figure 7). For the sake of space, a group analysis is performed

538     rather than a single subject analysis. *The approach of the small cube into near space* produces

539     widespread activations (Figure 7A). This network includes the orbitofrontal cortex (12, 46p),

540     prefrontal and premotor cortex (FEF, F4, F5), parietal cortex (VIP, PIP, 7a, 7b, 7ab), temporal

541     cortex (MT, MST, TPOr, IPa) and visual areas (V1, V2, V3). This network is mostly included

542     in the near space network (Figure 7A, black contours, Figure 3, top panel), though a

543     heterogeneity can be noted. Some cortical regions modulated by near space stimulations are

28

544    not activated by intrusion into near space, mostly along the ventral visual stream (Figure 7A,

545    uncolored cortex within the black contours). Other cortical regions modulated by near space

546    stimulations are equally activated by intrusion into near space and near space stimulations

547    (Figure 7A, colored activations within the black contours). Importantly, not all the regions

548    that are activated by intrusion into peripersonal space are also activated by the sustained

549    presence of a stimulus in near space (Figure 1D (7), Figure 7A, white contours outside the

550    black contours). *The approach of the big cube into far space* produced very similar activation

551    patterns to those observed during the approach of the small cube into near space, to the

552    notable exception of the orbitofrontal cortex, possibly indicating an emotional component to

553    intrusion into near space (Figure 7E). In contrast, *the approach of the small cube within far*

554    *space* produced more restricted activations, mostly in the intraparietal sulcus (IPS), in the

555    superior temporal sulcus (STS) as well as in the striate and extrastriate cortex (Figure 7C).

556    *When the small cube recedes from near space*, very few activations are observed,

557    circumscribed to the prefrontal area 46 and the superior temporal sulcus STS (Figure 7B). A

558    very similar activation pattern is described for *the recession of the small cube from far space*

559    (Figure 7D). Last, activations are more widespread for *the large cube receding from far*

560    *space*, quite close to those observed for the approach of this stimulus into far space (Figure

561    5F). This contrasts with the difference observed between the looming and recession of the

562    small cube in near space, and support the idea that the representation of object movement

563    vectors in the cortex differ depending on whether movement takes place in near or in far

564    space.

565

566    **Near to far coding gradient in the arcuate (AS) and intraparietal sulcus (IPS).**

567    Intraparietal and periarcuate regions have been shown to play a key role in space

568    representation and space representation for action. In this section, we focus on these two

29

569    regions (Figure 8). Again, for the sake of space, a group analysis is performed rather than a

570    single subject analysis. This group analysis captures the common activations already

571    described at the single individual level in figures 3, 4 and 5. In the *Arcuate sulcus*, near space

572    is specifically encoded by areas 46p, 12, F4, F5 and SEF whereas specific far space is overall

573    represented at the inferior tip of the AS and along the gyrus posterior to the AS. In the

574    *Intraparietal sulcus*, near space is specifically encoded by the VIP area and PGm area

575    whereas far space is specifically encoded by the areas 5v and PIP.

576        Different regions of interest were defined along the AS and the IPS, and the

577    percentage of signal change (PSC) within each of these ROIs was extracted for each contrast

578    of specific near space, preferential near space, unselective near and far space, preferential far

579    space or specific far space, Figure 8, histograms). Overall, this analysis confirms the

580    existence, along the AS, bilaterally, of a progressive increase in the PSC to far stimuli (central

581    blue bars) from ROIs 1 to 5 (176% of increase for the left and 151% for the right), together

582    with a quite stable PSC for near stimuli (central red bars). A similar progressive increase in

583    the PSC to far stimuli can also be observed in the IPS, bilaterally (ROIs 6 to 9, central blue

584    bars, 101% for the left and 112% for the right), together with a stable PSC for near stimuli

585    (central red bars). Confirming the whole brain contrast analysis, we also note deactivations or

586    non-significant activations during the stimulation of far space by a larger object in the specific

587    near space contrast (ROIs 1, 2 and 6, bilaterally) and the preferential near space contrast

588    (ROIs 3 and 7, bilaterally). Likewise, the PSC during the stimulation of far space by a larger

589    object are significantly higher than the PSC during the stimulation of near space in the

590    specific and preference contrasts (ROIs 5 and 9, bilaterally). In the unselective near and far

591    space contrast, the PSCs during the stimulation of near space and far space are not

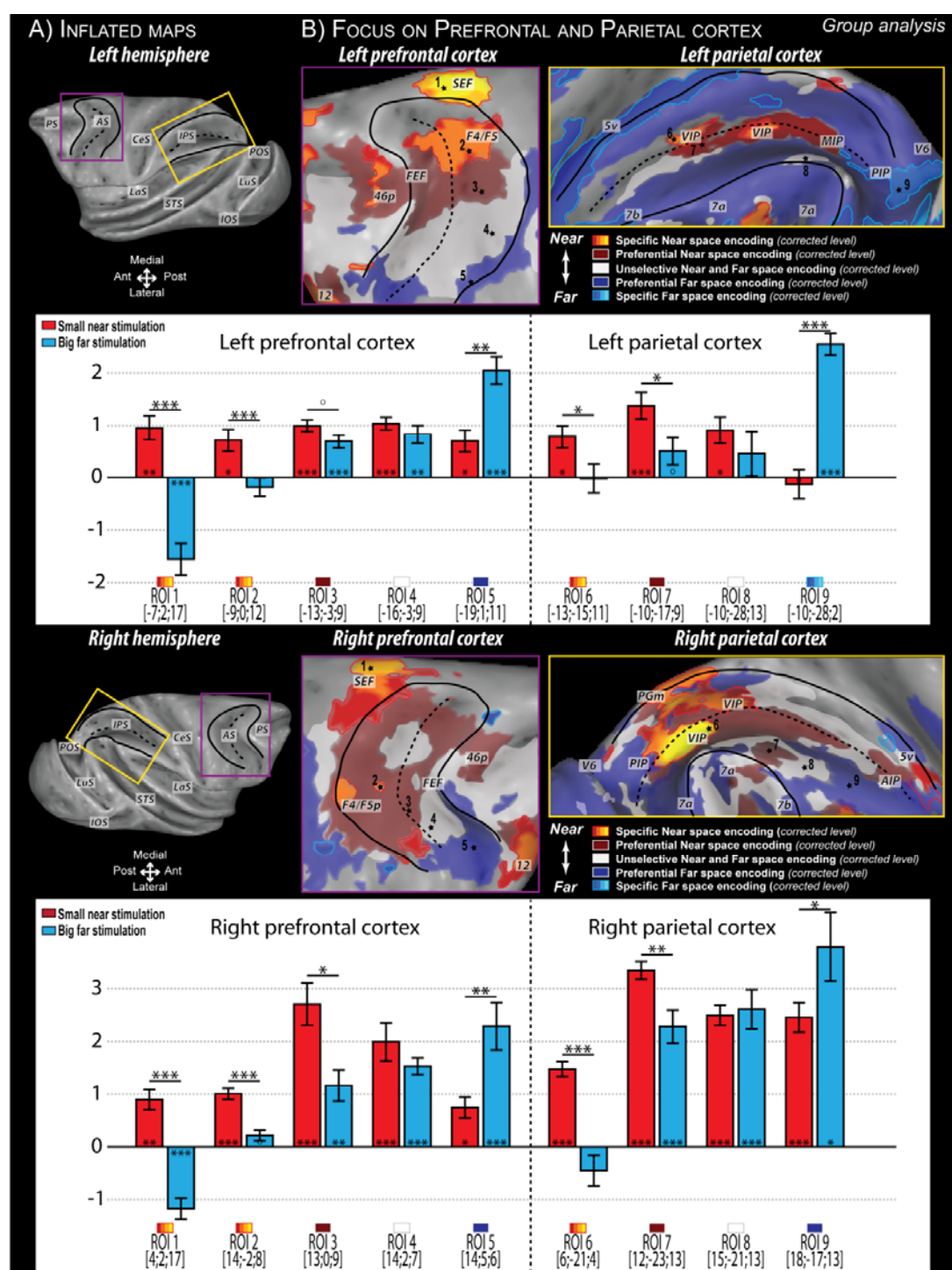592    significantly different (ROIs 4 and 8, bilaterally).

593

**Figure 8:** Near to Far coding gradient in the arcuate sulcus (AS) and the intraparietal

sulcus (IPS). A) Inflated representation of the cortex, (left and right hemisphere of the

reference monkey cortex). The purple inset corresponds to the AS and the yellow inset

corresponds to the IPS as represented in B). Black solid lines indicate the limit

598    between the convexity and the banks of the IPS and AS; black dashed lines indicated

599    the bottom of the sulcus. B) Prefrontal (purple inset) and parietal (yellow inset)

600    activations of near and far space networks (group analysis superimposing the

601    activations described in figure 4 and 5) on the same inflated maps, for the left and

602    right hemispheres. Red to yellow color scale: selective near space coding; Red:

603    preferential coding for near space; White: unselective coding for near and far space;

604    Blue: preferential coding for far space; Dark blue to light blue color scale: selective

605    near space coding. Gray regions correspond to regions activated neither by the large

606    stimulus in far space nor by the small stimulus in near space. 5v, ventral area 5v;

607    7a,7b/7ab, areas 7a, 7b or 7ab: MIP, medial intraparietal area MIP, V6: cortical visual

608    area V6. For other conventions, see Figure 3, 4 and 5. Five regions of interest were

609    defined along the AS and four along the IPS, and percentage of signal change (PSC)

610    within each of these ROIs was extracted for each contrast of specific near space,

611    preferential near space, unselective near and far space, preferential far space and

612    specific far space. Below each inflated map, the PSCs are plotted for the stimulation of

613    the small cube in the near space (orange bars) and for the stimulation of the big cube

614    on the far space (blue bars). The specific location of each ROI as well as the map they

615    belong to is indicated at the bottom of the figure. Statistical significance is represented

616    as follow: *$p<0.05$; **$p<0.01$; ***$<0.001$ (paired t-tests with Bonferroni correction);

617    **o** $p<0.05$ (paired t-tests).

618

619

620 **DISCUSSION**

621    In the following, we discuss in the identified primate networks associated with either

622    near or far space stimulation with naturalistic dynamic objects in the light of the related

623    literature.

624

625    **Near space specific cortical network**

626    The near space specific cortical network we describe here is surprisingly large. It

627    involves multisensory visuo-tactile cortical regions whose neurons have already been

628    described to encode nearby objects relative to the body and subserve peripersonal space

629    representation, namely parietal area VIP (Duhamel et al., 1997, 1998; Avillac et al., 2005;

630    Schlack et al., 2005; Bremmer et al., 2013; Guipponi et al., 2013) and premotor area F4

631    (Cléry et al., 2015b; Fogassi et al., 1996; Graziano et al., 1994, 1997, 1999; Matelli and

632    Luppino, 2001; Rizzolatti et al., 1981). These two regions have anatomical connections and

633    functional homologies. This VIP-F4 network processes all the necessary information to bind

634    together the localization of objects around our body with actions towards these objects and to

635    define a safety body margin contributing to the definition of self with respect to the external

636    world (Graziano and Cooke, 2006; Brozzoli et al., 2013, 2014; Chen et al., 2014; Cléry et al.,

637    2015b). In our study, area VIP is sensitive to dynamic stimuli in near space whereas a

638    previous study did not identify a sensitivity to the 3-dimensional structure of static stimuli in

639    VIP (Durand et al., 2007). In a more recent study and in agreement with our results, Van

640    Dromme et al., (2016) show that VIP is involved in depth-structure processing. On the other

641    hand, the parietal area AIP and premotor area F5, activated here by near space stimulations,

642    have been shown to be essential for grasping and reaching processing (Fogassi et al., 2001;

643    Gallese et al., 1994; Murata et al., 2000, 1997; Sakata and Taira, 1994). These two areas share

644    also strong anatomical connections and functional homologies and have consequently been

645    proposed to form a second parieto-premotor network dedicated for action (Gallese et al.,

646    1996; Iriki et al., 1996; Matelli and Luppino, 2001; Rizzolatti and Luppino, 2001; Rizzolatti

647    and Matelli, 2003; see for discussion Cléry et al., 2015b)(see for discussion Cléry et al.,

648    2015b; Gallese et al., 1996; Iriki et al., 1996; Matelli and Luppino, 2001; Rizzolatti and

649    Luppino, 2001; Rizzolatti and Matelli, 2003).

650        We also identify cortical areas whose contribution to near space processing has been

651    partly overlooked. We describe the involvement of dorsal premotor regions, in agreement

652    with the description, in patients with dorsolateral prefrontal cortex damage, of a near space

653    specific neglect (Aimola et al., 2012). We also describe the involvement of posterior, fundal

654    and medial parietal areas, in agreement with the description of a near space neglect in patients

655    with posterior parietal lesions (Halligan and Marshall, 1991). Near space activations are also

656    observed within the fundus of the STS and on the inferior temporal convexity, suggesting a

657    specific processing of near objects feature and identity within the ventral visual stream.

658        Near space specific activations are also observed in area SII, possibly revealing a

659    general "attention-to-touch" process due to the anticipation of tactile stimulation to the body.

660    This could also actuate the strong functional link between near space processing and the

661    somatosensory representation of self. While previous studies have mostly assumed that this

662    link is subserved by associative multisensory visuo-tactile areas (Blanke, 2012; Makin et al.,

663    2008), the present observations suggest that low level sensory areas might also be involved in

664    the representation of space at the frontier of self. Close to the face, the moving cube can be

665    viewed as a potentially dangerous object. This could possibly also account for the observed

666    orbitofrontal activations (area 12, Murray and Izquierdo 2007).

667        Overall, the non-human near space specific cortical network we describe here has

668    major specificities as compared to the analog human network. We essentially describe

669    bilateral cortical regions, while in humans, only the left dorsal occipital cortex, the left

670    intraparietal and the left ventral premotor appear to be involved in near space processing

671    (Aimola et al., 2012; Weiss et al., 2000). This near space network areas also appears larger in

672    the monkeys than in humans. This could be due to the fact that we stimulated near space at

673    15cm away from the subject while Weiss et al. (2000)used stimulations at 70cm.

674    Alternatively, this could be a genuine interspecies difference.

675

**Far space specific cortical network**

677    The observed monkey far space specific cortical network is also very extended,

678    involving large portions of the occipital cortex, posterior temporal and superior temporal

679    regions, similar to what is seen in humans (Weiss et al. (2000). This is in agreement with the

680    far space neglect following a temporal hematoma (Vuilleumier et al., 1998).

681    In our study, we show a clear far space preference coding in V6A. A human study

682    (Quinlan and Culham, 2007) shows a near preference coding in dPOS. This is suprising given

683    the high degree of similarity between the human superior parieto-occipital cortex (sPOC) and the

684    macaque parieto-occipital area including areas V6 and V6A (Galletti et al., 1999, 2005). This

685    discrepancy can be explained by important experimental differences. Whereas we use naturalistic

686    and dynamic stimuli in near or far space while monkeys fixated an intermediate position, in

687    Quinlan and Culham (2007), participants fixated in near vs. far space with no other visual

688    stimulation. Therefore, only oculomotor signals of vergence eye position and ocular

689    accommodation are manipulated by the task design.

690    Last, Rizzolatti et al. (1983) describe a more pronounced hemineglect in far than in

691    near space following prearcuate area 8 ablations whereas we describe a preferential though

692    not specific coding for near space in this region. This discrepancy could reflect a task

693    dependence of far and near space processing as described in humans, in active oculomotor or

694    reaching contexts (Aimola et al., 2012; Keller et al., 2005).

695

696    **Object size effects**

697    All the cortical regions involved in processing the small object in far space also

698    contribute to the processing of the large object in far space. The reverse is not true. At the

699    neuronal level, this possibly suggests a multiplexing of object real-size and location in far

700    space relative to the subject, as a big object is not expected to have the same valence as a

701    small object in far space. Size coding might further be normalized with respected to the actual

702    body size of the subject, big objects being possibly more dangerous for small individuals than

703    for larger individuals.

704    Human studies show that visual objects may be mapped along the ventral occipito-

705    temporal cortex according to their real-world size, reflecting the visual or functional

706    properties associated with small versus big real-world objects (Konkle and Oliva, 2012) but

707    also abstract and conceptual size representation (Gabay et al., 2016). It would be highly

708    interesting to test different objects with real-world size well known for monkey to further

709    characterize the interaction between real object-size and object distance from the subject.

710

711    **Looming stimuli and peripersonal space**

712    The looming of the small cube in near space results in large activations involving both

713    the near and far space networks. Such looming stimuli have been described to trigger

714    stereotyped defense responses and enhance reaction times or sensitivity to a second stimulus

715    (Schiff et al., 1962; Ball and Tronick, 1971; Vagnoni et al., 2012; Canzoneri et al., 2012;

716    Kandula et al., 2015; Cléry et al., 2015a) including nociceptive stimuli (De Paepe et al.,

717    2016). Recently, we have described that this type of dynamic visual stimuli activate a parieto-

718    frontal network highly overlapping with the one described here (Cléry et al., 2015b,

719    2017)(Cléry et al., 2017, 2015b). This functional overlap between a network encoding the

720    presence of a stimulus within peripersonal space at the same time as intrusion into

721    peripersonal space reinforces the view that this network encodes visual stimuli in relation with

722    the margin of self and their possible tactile consequences on the body.

723

724    **Substrates for dynamic space representation**

725    The description of specific networks for near and far space processing should not have

726    us overlook the fact that large cortical regions contribute to the processing of both far and

727    near objects, though often favoring one over the other as in LIP, 7a or 7b. Bimodal visuo-

728    tactile neurons have been described in area 7b with large receptive fields over the arm, leg,

729    chest or whole body (Leinonen et al., 1979). Lesions of this region induce a neglect in

730    peripersonal space (Matelli et al., 1984), suggesting that area 7b is involved in the perception

731    of near space and in the organization of movements towards stimuli presented in peripersonal

732    space. However, we found a privileged coding of far space for this area, calling for

733    reassessment of its functional role in relation with space processing.

734    The description of large cortical regions having either a preference for near or far

735    space processing call for reappraising far space or near space specificity. Indeed, the

736    alternative view we would like to suggest is that of a continuous encoding of relative distance

737    to the body, in the form of a far-to-near gradient. In this context, far or near space specific

738    regions represent the extreme points of this continuum. The idea of such a continuum is

739    supported by the fact that no abrupt change in visuo-spatial neglect can be seen between near

740    and far space (Cowey et al., 1999). Another indirect evidence can be found in a recent non-

741    human fMRI study (Joly et al., 2009), which describes disparity-related signals in far space in

742    area F5a, close to periarcuate far space activation in our Figure 8. It is important to note that

37

743    the existence of such a cortical far-to-near gradient in space representation does not preclude

744    the existence of a physically delineable peripersonal space (Berti and Frassinetti 2000;

745    Macaluso and Maravita 2010; Farnè et al. 2005; Ladavas and Serino 2008).

746        Our results open the way to study how these two networks dynamically interact during

747    action planning, tool use or as a function of the emotional or social contexts as some studies

748    show that these processes are dynamics (Markman and Brendl, 2005; Bassolino et al., 2010;

749    Brozzoli et al., 2010; Lourenco and Longo, 2009; Lourenco et al., 2011; Valdés-Conroy et al.,

750    2012; Teneggi et al., 2013).

751

755

## Bibliography

757    Aimola, L., Schindler, I., Venneri, A., 2012. Task- and response related dissociations
758    between neglect in near and far space: a morphometric case study. Behav Neurol 27, 245–
759    257. https://doi.org/10.3233/BEN-2012-110243

760    Avillac, M., Denève, S., Olivier, E., Pouget, A., Duhamel, J.-R., 2005. Reference frames
761    for representing visual and tactile locations in parietal cortex. Nat Neurosci 8, 941–949.
762    https://doi.org/10.1038/nn1480

763    Avillac, M., Hamed, S.B., Duhamel, J.-R., 2007. Multisensory Integration in the Ventral
764    Intraparietal Area of the Macaque Monkey. J. Neurosci. 27, 1922–1932.
765    https://doi.org/10.1523/JNEUROSCI.2646-06.2007

766    Avillac, M., Olivier, E., Denève, S., Ben Hamed, S., Duhamel, J.-R., 2004. Multisensory
767    integration in multiple reference frames in the posterior parietal cortex. Cognitive Processing
768    5, 159–166. https://doi.org/10.1007/s10339-004-0021-3

769    Ball, W., Tronick, E., 1971. Infant responses to impending collision: optical and real.
770    Science 171, 818–820.

771    Bassolino, M., Serino, A., Ubaldi, S., Làdavas, E., 2010. Everyday use of the computer
772    mouse extends peripersonal space representation. Neuropsychologia 48, 803–811.

773     https://doi.org/10.1016/j.neuropsychologia.2009.11.009

774     Berti, A., Frassinetti, F., 2000. When far becomes near: remapping of space by tool use. J
775     Cogn Neurosci 12, 415–420.

776     Blanke, O., 2012. Multisensory brain mechanisms of bodily self-consciousness. Nat. Rev.
777     Neurosci. 13, 556–571. https://doi.org/10.1038/nrn3292

778     Bremmer, F., Duhamel, J.-R., Ben Hamed, S., Graf, W., 2002a. Heading encoding in the
779     macaque ventral intraparietal area (VIP). European Journal of Neuroscience 16, 1554–1568.
780     https://doi.org/10.1046/j.1460-9568.2002.02207.x

781     Bremmer, F., Duhamel, J.R., Ben Hamed, S., Graf, W., 2000. Stages of self-motion
782     processing in primate posterior parietal cortex. Int. Rev. Neurobiol. 44, 173–198.

783     Bremmer, F., Duhamel, J.-R., Ben Hamed, S., Graf, W., 1997. The representation of
784     movement in near extra-personal space in the macaque ventral intraparietal area (VIP)., in:
785     Thier, P., Karnath, H.-O. (Eds.), Parietal Lobe Contributions to Orientation in 3D Space,
786     Experimental Brain Research Series, Vol 25. Springer, pp. 619–630.

787     Bremmer, F., Klam, F., Duhamel, J.-R., Ben Hamed, S., Graf, W., 2002b. Visual–
788     vestibular interactive responses in the macaque ventral intraparietal area (VIP). European
789     Journal of Neuroscience 16, 1569–1586. https://doi.org/10.1046/j.1460-9568.2002.02206.x

790     Bremmer, F., Schlack, A., Kaminiarz, A., Hoffmann, K.P., 2013. Encoding of movement
791     in near extrapersonal space in primate area VIP. Front. Behav. Neurosci 7, 8.
792     https://doi.org/10.3389/fnbeh.2013.00008

793     Brett, M., Anton, J.-L., Valabregue, R., Poline, J.-B., 2002. Region of interest analysis
794     using the MarsBar toolbox for SPM 99. Presented at the 8th International Conference on
795     Functional Mapping of the Human Brain (June 2–6, 2002, Sendai, Japan), 16, S497.

796     Brozzoli, C., Cardinali, L., Pavani, F., Farnè, A., 2010. Action-specific remapping of
797     peripersonal        space.        Neuropsychologia        48,        796–802.
798     https://doi.org/10.1016/j.neuropsychologia.2009.10.009

799     Brozzoli, C., Ehrsson, H.H., Farnè, A., 2014. Multisensory representation of the space near
800     the hand: from perception to action and interindividual interactions. Neuroscientist 20, 122–
801     135. https://doi.org/10.1177/1073858413511153

802     Brozzoli, C., Gentile, G., Bergouignan, L., Ehrsson, H.H., 2013. A Shared Representation
803     of the Space Near Oneself and Others in the Human Premotor Cortex. Current Biology 23,
804     1764–1768. https://doi.org/10.1016/j.cub.2013.07.004

805     Canzoneri, E., Magosso, E., Serino, A., 2012. Dynamic Sounds Capture the Boundaries of
806     Peripersonal    Space    Representation    in    Humans.    PLoS    ONE    7,    e44306.
807     https://doi.org/10.1371/journal.pone.0044306

808     Chen, X., Sanayei, M., Thiele, A., 2014. Stimulus Roving and Flankers Affect Perceptual
809     Learning of Contrast Discrimination in Macaca mulatta. PLoS ONE 9, e109604.

810     https://doi.org/10.1371/journal.pone.0109604

811     Cléry, J., Guipponi, O., Odouard, S., Pinède, S., Wardak, C., Hamed, S.B., 2017. The
812     Prediction of Impact of a Looming Stimulus onto the Body Is Subserved by Multisensory
813     Integration          Mechanisms.          J.          Neurosci.          37,          10656–10670.
814     https://doi.org/10.1523/JNEUROSCI.0610-17.2017

815     Cléry, J., Guipponi, O., Odouard, S., Wardak, C., Ben Hamed, S., 2015a. Impact prediction
816     by looming visual stimuli enhances tactile detection. J. Neurosci. 35, 4179–4189.
817     https://doi.org/10.1523/JNEUROSCI.3031-14.2015

818     Cléry, J., Guipponi, O., Wardak, C., Ben Hamed, S., 2015b. Neuronal bases of
819     peripersonal and extrapersonal spaces, their plasticity and their dynamics: Knowns and
820     unknowns.              Neuropsychologia              70,              313–326.
821     https://doi.org/10.1016/j.neuropsychologia.2014.10.022

822     Cowey, A., Small, M., Ellis, S., 1999. No abrupt change in visual hemineglect from near to
823     far space. Neuropsychologia 37, 1–6.

824     Cowey, A., Small, M., Ellis, S., 1994. Left visuo-spatial neglect can be worse in far than in
825     near space. Neuropsychologia 32, 1059–1066.

826     De Paepe, A.L., Crombez, G., Legrain, V., 2016. What's Coming Near? The Influence of
827     Dynamical Visual Stimuli on Nociceptive Processing. PLOS ONE 11, e0155864.
828     https://doi.org/10.1371/journal.pone.0155864

829     Duhamel, J.-R., Bremmer, F., BenHamed, S., Graf, W., 1997. Spatial invariance of visual
830     receptive      fields      in      parietal      cortex      neurons.      Nature      389,      845–848.
831     https://doi.org/10.1038/39865

832     Duhamel, J.-R., Colby, C.L., Goldberg, M.E., 1998. Ventral Intraparietal Area of the
833     Macaque: Congruent Visual and Somatic Response Properties. Journal of Neurophysiology
834     79, 126–136.

835     Durand, J.-B., Nelissen, K., Joly, O., Wardak, C., Todd, J.T., Norman, J.F., Janssen, P.,
836     Vanduffel, W., Orban, G.A., 2007. Anterior regions of monkey parietal cortex process visual
837     3D shape. Neuron 55, 493–505. https://doi.org/10.1016/j.neuron.2007.06.040

838     Durand, J.-B., Peeters, R., Norman, J.F., Todd, J.T., Orban, G.A., 2009. Parietal regions
839     processing visual 3D shape extracted from disparity. NeuroImage 46, 1114–1126.
840     https://doi.org/10.1016/j.neuroimage.2009.03.023

841     Everling, S., Munoz, D.P., 2000. Neuronal Correlates for Preparatory Set Associated with
842     Pro-Saccades and Anti-Saccades in the Primate Frontal Eye Field. J. Neurosci. 20, 387–400.

843     Fize, D., Vanduffel, W., Nelissen, K., Denys, K., d'Hotel, C.C., Faugeras, O., Orban, G.A.,
844     2003. The Retinotopic Organization of Primate Dorsal V4 and Surrounding Areas: A
845     Functional Magnetic Resonance Imaging Study in Awake Monkeys. J. Neurosci. 23, 7395–
846     7406.

847    Fogassi, L., Gallese, V., Buccino, G., Craighero, L., Fadiga, L., Rizzolatti, G., 2001.
848    Cortical mechanism for the visual guidance of hand grasping movements in the monkeyA
849    reversible inactivation study. Brain 124, 571–586. https://doi.org/10.1093/brain/124.3.571

850    Fogassi, L., Gallese, V., Fadiga, L., Luppino, G., Matelli, M., Rizzolatti, G., 1996. Coding
851    of peripersonal space in inferior premotor cortex (area F4). J. Neurophysiol. 76, 141–157.

852    Gabay, S., Kalanthroff, E., Henik, A., Gronau, N., 2016. Conceptual size representation in
853    ventral       visual       cortex.       Neuropsychologia       81,       198–206.
854    https://doi.org/10.1016/j.neuropsychologia.2015.12.029

855    Gallese, V., Fadiga, L., Fogassi, L., Rizzolatti, G., 1996. Action recognition in the
856    premotor cortex. Brain 119, 593–609. https://doi.org/10.1093/brain/119.2.593

857    Gallese, V., Murata, A., Kaseda, M., Niki, N., Sakata, H., 1994. Deficit of hand preshaping
858    after muscimol injection in monkey parietal cortex. Neuroreport 5, 1525–1529.

859    Galletti, C., Fattori, P., Gamberini, M., Kutz, D.F., 1999. The cortical visual area V6: brain
860    location and visual topography. European Journal of Neuroscience 11, 3922–3936.
861    https://doi.org/10.1046/j.1460-9568.1999.00817.x

862    Galletti, C., Gamberini, M., Kutz, D.F., Baldinotti, I., Fattori, P., 2005. The relationship
863    between V6 and PO in macaque extrastriate cortex. European Journal of Neuroscience 21,
864    959–970. https://doi.org/10.1111/j.1460-9568.2005.03911.x

865    Gentilucci, M., Fogassi, L., Luppino, G., Matelli, M., Camarda, R., Rizzolatti, G., 1988.
866    Functional organization of inferior area 6 in the macaque monkey. I. Somatotopy and the
867    control of proximal movements. Exp Brain Res 71, 475–490.

868    Graziano, M.S., Yap, G.S., Gross, C.G., 1994. Coding of visual space by premotor
869    neurons. Science 266, 1054–1057.

870    Graziano, M.S.A., Cooke, D.F., 2006. Parieto-frontal interactions, personal space, and
871    defensive        behavior.       Neuropsychologia       44,       845–859.
872    https://doi.org/10.1016/j.neuropsychologia.2005.09.009

873    Graziano, M.S.A., Hu, X.T., Gross, C.G., 1997. Visuospatial Properties of Ventral
874    Premotor Cortex. Journal of Neurophysiology 77, 2268–2292.

875    Graziano, M.S.A., Reiss, L.A.J., Gross, C.G., 1999. A neuronal representation of the
876    location of nearby sounds. Nature 397, 428–430. https://doi.org/10.1038/17115

877    Gross, C.G., Graziano, M.S.A., 1995. REVIEW ■□: Multiple Representations of Space in
878    the Brain. Neuroscientist 1, 43–50. https://doi.org/10.1177/107385849500100107

879    Guipponi, O., Cléry, J., Odouard, S., Wardak, C., Ben Hamed, S., 2015a. Whole brain
880    mapping of visual and tactile convergence in the macaque monkey. NeuroImage 117, 93–102.
881    https://doi.org/10.1016/j.neuroimage.2015.05.022

882    Guipponi, O., Odouard, S., Pinède, S., Wardak, C., Ben Hamed, S., 2015b. fMRI Cortical

883    Correlates of Spontaneous Eye Blinks in the Nonhuman Primate. Cereb. Cortex 25, 2333–
884    2345. https://doi.org/10.1093/cercor/bhu038

885    Guipponi, O., Wardak, C., Ibarrola, D., Comte, J.-C., Sappey-Marinier, D., Pinède, S.,
886    Hamed, S.B., 2013. Multimodal Convergence within the Intraparietal Sulcus of the Macaque
887    Monkey. J. Neurosci. 33, 4128–4139. https://doi.org/10.1523/JNEUROSCI.1421-12.2013

888    Halligan, P.W., Marshall, J.C., 1991. Left neglect for near but not far space in man. Nature
889    350, 498–500. https://doi.org/10.1038/350498a0

890    Hutchison, R.M., Gallivan, J.P., Culham, J.C., Gati, J.S., Menon, R.S., Everling, S., 2012.
891    Functional connectivity of the frontal eye fields in humans and macaque monkeys
892    investigated with resting-state fMRI. Journal of Neurophysiology 107, 2463–2474.
893    https://doi.org/10.1152/jn.00891.2011

894    Hyvärinen, J., Poranen, A., 1974. Function of the parietal associative area 7 as revealed
895    from cellular discharges in alert monkeys. Brain 97, 673–692.

896    Iriki, A., Tanaka, M., Iwamura, Y., 1996. Coding of modified body schema during tool use
897    by macaque postcentral neurones. Neuroreport 7, 2325–2330.

898    Joly, O., Vanduffel, W., Orban, G.A., 2009. The monkey ventral premotor cortex
899    processes    3D    shape    from    disparity.    NeuroImage    47,    262–272.
900    https://doi.org/10.1016/j.neuroimage.2009.04.043

901    Kandula, M., Hofman, D., Dijkerman, H.C., 2015. Visuo-tactile interactions are dependent
902    on the predictive value of the visual stimulus. Neuropsychologia 70, 358–366.
903    https://doi.org/10.1016/j.neuropsychologia.2014.12.008

904    Keller, I., Schindler, I., Kerkhoff, G., von Rosen, F., Golz, D., 2005. Visuospatial neglect
905    in near and far space: dissociation between line bisection and letter cancellation.
906    Neuropsychologia 43, 724–731. https://doi.org/10.1016/j.neuropsychologia.2004.08.003

907    Kolster, H., Janssens, T., Orban, G.A., Vanduffel, W., 2014. The Retinotopic Organization
908    of Macaque Occipitotemporal Cortex Anterior to V4 and Caudoventral to the Middle
909    Temporal    (MT)    Cluster.    J.    Neurosci.    34,    10168–10191.
910    https://doi.org/10.1523/JNEUROSCI.3288-13.2014

911    Konkle, T., Oliva, A., 2012. A Real-World Size Organization of Object Responses in
912    Occipitotemporal    Cortex.    Neuron    74,    1114–1124.
913    https://doi.org/10.1016/j.neuron.2012.04.036

914    Koyama, M., Hasegawa, I., Osada, T., Adachi, Y., Nakahara, K., Miyashita, Y., 2004.
915    Functional Magnetic Resonance Imaging of Macaque Monkeys Performing Visually Guided
916    Saccade Tasks: Comparison of Cortical Eye Fields with Humans. Neuron 41, 795–807.
917    https://doi.org/10.1016/S0896-6273(04)00047-9

918    Leinonen, L., Hyvärinen, J., Nyman, G., Linnankoski, I., 1979. I. Functional properties of
919    neurons in lateral part of associative area 7 in awake monkeys. Exp Brain Res 34, 299–320.

920     Lewis, J.W., Van Essen, D.C., 2000. Corticocortical connections of visual, sensorimotor,
921     and multimodal processing areas in the parietal lobe of the macaque monkey. J. Comp.
922     Neurol.   428,   112–137.   https://doi.org/10.1002/1096-9861(20001204)428:1<112::AID-
923     CNE8>3.0.CO;2-9

924     Lourenco, S.F., Longo, M.R., 2009. The plasticity of near space: evidence for contraction.
925     Cognition 112, 451–456. https://doi.org/10.1016/j.cognition.2009.05.011

926     Lourenco, S.F., Longo, M.R., Pathman, T., 2011. Near space and its relation to
927     claustrophobic fear. Cognition 119, 448–453. https://doi.org/10.1016/j.cognition.2011.02.009

928     Macaluso, E., Maravita, A., 2010. The representation of space near the body through touch
929     and         vision.         Neuropsychologia         48,         782–795.
930     https://doi.org/10.1016/j.neuropsychologia.2009.10.010

931     Makin, T.R., Holmes, N.P., Ehrsson, H.H., 2008. On the other hand: dummy hands and
932     peripersonal space. Behav. Brain Res. 191, 1–10. https://doi.org/10.1016/j.bbr.2008.02.041

933     Mandeville, J.B., Choi, J.-K., Jarraya, B., Rosen, B.R., Jenkins, B.G., Vanduffel, W., 2011.
934     FMRI of cocaine self-administration in macaques reveals functional inhibition of basal
935     ganglia. Neuropsychopharmacology 36, 1187–1198. https://doi.org/10.1038/npp.2011.1

936     Markman, A.B., Brendl, C.M., 2005. Constraining theories of embodied cognition. Psychol
937     Sci 16, 6–10. https://doi.org/10.1111/j.0956-7976.2005.00772.x

938     Matelli, M., Gallese, V., Rizzolatti, G., 1984. [Neurological deficit following a lesion in
939     the parietal area 7b in the monkey]. Boll. Soc. Ital. Biol. Sper. 60, 839–844.

940     Matelli, M., Luppino, G., 2001. Parietofrontal Circuits for Action and Space Perception in
941     the Macaque Monkey. NeuroImage 14, S27–S32. https://doi.org/10.1006/nimg.2001.0835

942     Murata, A., Fadiga, L., Fogassi, L., Gallese, V., Raos, V., Rizzolatti, G., 1997. Object
943     representation in the ventral premotor cortex (area F5) of the monkey. J. Neurophysiol. 78,
944     2226–2230.

945     Murata, A., Gallese, V., Luppino, G., Kaseda, M., Sakata, H., 2000. Selectivity for the
946     shape, size, and orientation of objects for grasping in neurons of monkey parietal area AIP. J.
947     Neurophysiol. 83, 2580–2601. https://doi.org/10.1152/jn.2000.83.5.2580

948     Murray, E.A., Izquierdo, A., 2007. Orbitofrontal cortex and amygdala contributions to
949     affect   and   action   in   primates.   Ann.   N.   Y.   Acad.   Sci.   1121,   273–296.
950     https://doi.org/10.1196/annals.1401.021

951     Nelissen, K., Joly, O., Durand, J.-B., Todd, J.T., Vanduffel, W., Orban, G.A., 2009. The
952     Extraction of Depth Structure from Shading and Texture in the Macaque Brain. PLoS One 4.
953     https://doi.org/10.1371/journal.pone.0008306

954     Paxinos, G., Huang, X.-F., Toga, A., 2000. The Rhesus Monkey Brain in Stereotaxic
955     Coordinates. Faculty of Health and Behavioural Sciences - Papers (Archive).

956    Quinlan, D.J., Culham, J.C., 2007. fMRI reveals a preference for near viewing in the
957    human        parieto-occipital        cortex.        NeuroImage        36,        167–187.
958    https://doi.org/10.1016/j.neuroimage.2007.02.029

959    Rizzolatti, G., Luppino, G., 2001. The Cortical Motor System. Neuron 31, 889–901.
960    https://doi.org/10.1016/S0896-6273(01)00423-8

961    Rizzolatti, G., Matelli, M., 2003. Two different streams form the dorsal visual system:
962    anatomy and functions. Exp Brain Res 153, 146–157. https://doi.org/10.1007/s00221-003-
963    1588-0

964    Rizzolatti, G., Matelli, M., Pavesi, G., 1983. Deficits in attention and movement following
965    the removal of postarcuate (area 6) and prearcuate (area 8) cortex in macaque monkeys. Brain
966    106 (Pt 3), 655–673.

967    Rizzolatti, G., Scandolara, C., Matelli, M., Gentilucci, M., 1981. Afferent properties of
968    periarcuate neurons in macaque monkeys. II. Visual responses. Behav. Brain Res. 2, 147–163.

969    Sakata, H., Taira, M., 1994. Parietal control of hand action. Current Opinion in
970    Neurobiology 4, 847–856. https://doi.org/10.1016/0959-4388(94)90133-3

971    Schiff, W., Caviness, J.A., Gibson, J.J., 1962. Persistent fear responses in rhesus monkeys
972    to the optical stimulus of "looming." Science 136, 982–983.

973    Schlack, A., Sterbing-D'Angelo, S.J., Hartung, K., Hoffmann, K.-P., Bremmer, F., 2005.
974    Multisensory space representations in the macaque ventral intraparietal area. J. Neurosci. 25,
975    4616–4625. https://doi.org/10.1523/JNEUROSCI.0455-05.2005

976    Teneggi, C., Canzoneri, E., di Pellegrino, G., Serino, A., 2013. Social modulation of
977    peripersonal        space        boundaries.        Curr.        Biol.        23,        406–411.
978    https://doi.org/10.1016/j.cub.2013.01.043

979    Vagnoni, E., Lourenco, S.F., Longo, M.R., 2012. Threat modulates perception of looming
980    visual stimuli. Current Biology 22, R826–R827. https://doi.org/10.1016/j.cub.2012.07.053

981    Valdés-Conroy, B., Román, F.J., Hinojosa, J.A., Shorkey, S.P., 2012. So far so good:
982    emotion    in    the    peripersonal/extrapersonal    space.    PLoS    ONE    7,    e49162.
983    https://doi.org/10.1371/journal.pone.0049162

984    Van Dromme, I.C., Premereur, E., Verhoef, B.-E., Vanduffel, W., Janssen, P., 2016.
985    Posterior Parietal Cortex Drives Inferotemporal Activations During Three-Dimensional
986    Object Vision. PLOS Biology 14, e1002445. https://doi.org/10.1371/journal.pbio.1002445

987    Van Essen, D.C., Drury, H.A., Dickson, J., Harwell, J., Hanlon, D., Anderson, C.H., 2001.
988    An integrated software suite for surface-based analyses of cerebral cortex. J Am Med Inform
989    Assoc 8, 443–459.

990    Vanduffel, W., Fize, D., Mandeville, J.B., Nelissen, K., Van Hecke, P., Rosen, B.R.,
991    Tootell, R.B.H., Orban, G.A., 2001. Visual Motion Processing Investigated Using Contrast
992    Agent-Enhanced    fMRI    in    Awake    Behaving    Monkeys.    Neuron    32,    565–577.

993 https://doi.org/10.1016/S0896-6273(01)00502-5

994 Vuilleumier, P., Valenza, N., Mayer, E., Reverdin, A., Landis, T., 1998. Near and far
995 visual space in unilateral neglect. Ann. Neurol. 43, 406–410.
996 https://doi.org/10.1002/ana.410430324

997 Wardak, C., Guipponi, O., Pinède, S., Hamed, S.B., 2016. Tactile representation of the
998 head and shoulders assessed by fMRI in the nonhuman primate. Journal of Neurophysiology
999 115, 80–91. https://doi.org/10.1152/jn.00633.2015

1000 Weiss, P.H., Marshall, J.C., Wunderlich, G., Tellmann, L., Halligan, P.W., Freund, H.J.,
1001 Zilles, K., Fink, G.R., 2000. Neural consequences of acting in near versus far space: a
1002 physiological basis for clinical dissociations. Brain 123 Pt 12, 2531–2541.

1003 Womelsdorf, T., Everling, S., 2015. Long-Range Attention Networks: Circuit Motifs
1004 Underlying Endogenously Controlled Stimulus Selection. Trends in Neurosciences 38, 682–
1005 700. https://doi.org/10.1016/j.tins.2015.08.009

1006

1007 **Figure Legends**

1008 **Figure 1:** Experimental fMRI protocol. A) 3D naturalistic stimuli, a large 30x30x30 cm3

1009 cube and an identical small 3x3x3 cm3 cube. The 6 faces of each transparent cube were

1010 decorated with 6 different fractal images. B) Block design. C) Experimental set up. Near

1011 space (15 cm from the monkey's face) and far space (150 cm from the monkey's face) were

1012 stimulated with the two types of 3D stimuli (same apparent sizes). Fixation is achieved at an

1013 intermediate position (red fixation LED, at 90cm). D) Summary of contrast analyses

1014 performed to extract the networks of interest: condition of interest higher than fixation (first

1015 column), preferential coding of condition of interest (second column) and selective coding of

1016 condition of interest (third column).

1017

1018 **Figure 2:** Analysis of eye movements as function of stimulation blocks. 2A) X and 2B) Y eye

1019 traces for an exemplar run. 2C) Average and standard deviation of microsaccade and saccade

1020     duration with respect to the total blocks duration over all sessions (Kruskall-wallis: p<0.001

1021     for MZ and p<0.01 for MT).

1022

1023     **Figure 3:** Near space and far space individual analyses. Activations are presented on the

1024     flattened representation of the two monkey right and left hemispheres obtained with Caret.

1025     The upper part of the figure shows the near space stimulated with the small cube (SN) versus

1026     fixation contrast (t scores = 4.8 at p<0.05, FWE-corrected level in the red scale). Middle and

1027     lower panels present the far space respectively stimulated with the big (BF) and the small

1028     cubes (SF; t scores = 4.8 at p<0.05, FWE-corrected level respectively in the blue and green

1029     scales). The right panel represents selected coronal slices showing the activated areas for each

1030     contrast in both monkeys. A, Anterior; D, Dorsal; SN: small near; BF: big far; SF: small far.

1031     12, area 12; 45B, area 45B; 46, area 46; AIP, anterior intraparietal area AIP; CIP caudal

1032     intraparietal area; F2, premotor area F2; FEF, frontal eye field; LIP, lateral intraparietal area

1033     LIP; MT/MST, medial/superior temporal areas MT/MST; F4/F5, premotor areas F4/F5; PGm,

1034     medial parietal area PGm; PIP, posterior intraparietal area PIP, S2, somatosensory area 2;

1035     SEF: supplementary eye field; TPOr, rostral temporoparietal occipital area TPOr; VIP, ventral

1036     intraparietal area VIP; V1/V2/V3/V4, visual areas V1,V2,V3 or V4. Cortical sulci: AS,

1037     arcuate sulcus; CgS, cingulate sulcus; CeS, central sulcus; IOS, inferior occipital sulcus; IPS,

1038     intraparietal sulcus; LaS, lateral (Sylvian) sulcus; LuS, lunate sulcus; OTS, occipital temporal

1039     sulcus; POS, parieto-occipital sulcus; PS, principal sulcus; STS, superior temporal sulcus.

1040

1041     **Figure 4:** Non-selective, preferential and specific near space networks. Activations are

1042     presented on the flattened maps of individual monkeys. Only the key activations identified in

1043     three hemispheres out of four are labelled. A and C) Non-selective and preferential near space

1044     encoding for monkey Z (A) and T (C). Preferential near space coding corresponds to the

46

1045     cortical regions whose activations are higher for the small cube in near space than for the

1046     large cube in far space (t scores = 4.8 at p<0.05, FWE-corrected level in the dark red). B and

1047     D) Non-selective and specific near space encoding for monkey Z (B) and T (D). Specific near

1048     space encoding corresponds to the cortical regions which are activated by the small near cube

1049     but not for the large far cube (red to yellow scale, exclusive mask for far space versus fixation

1050     baseline applied at FWE-corrected level p<0.05). The outer red contours correspond to non-

1051     selective near space encoding (near space versus fixation, as in figure 3). For other

1052     conventions, see Figure 3.

1053

1054     **Figure 5:** Non-selective, preferential and specific far space networks. Activations are

1055     presented on the flattened maps of individual monkeys. Only the key activations identified in

1056     three hemispheres out of four are labelled. A and C) Non-selective and preferential far space

1057     encoding for monkey Z (A) and T (C). Preferential far space coding corresponds to the

1058     cortical regions whose activations are higher for the large cube in far space than for the small

1059     cube in near space (t scores = 4.8 at p<0.05, FWE-corrected level in the dark blue). B and D)

1060     Non-selective and specific far space encoding for monkey Z (B) and T (D). Specific far space

1061     encoding corresponds to the cortical regions which are activated by the large far cube but not

1062     for the small near cube (dark blue to light blue color scale, exclusive mask for near space

1063     versus fixation baseline applied at FWE-corrected level p<0.05). The outer blue contours

1064     correspond to non-selective far space encoding (far space versus fixation, as in figure 2). For

1065     other conventions, see Figure 3.

1066

1067     **Figure 6:** Preferential and specific encoding of the large cube in the far space. Activations are

1068     presented on the flattened maps of the reference monkey cortex (group analysis). Preferential

1069     encoding of the large cube in the far space corresponds to the cortical regions whose

47

1070 activations are higher for the big cube in far space than for the small cube in far space (t

1071 scores = 4.8 at p<0.05, FWE-corrected level in the dark blue). Specific encoding of the large

1072 cube in the far space corresponds to the cortical regions which are activated by the big cube

1073 but not for the small far cube in the far space (dark blue to light blue color scale, exclusive

1074 mask for the big cube in far space versus fixation baseline applied at FWE-corrected level

1075 p<0.05). For other conventions, see Figure 3.

1076

1077 **Figure 7:** Looming stimuli activate both Near and Far space network. Activations are

1078 presented on the flattened maps of the reference monkey cortex (group analysis). A, C and E,

1079 this presents the approach of the stimulus respectively towards near space with the small cube,

1080 towards far space with the small cube or towards far space with the big cube versus fixation

1081 contrast (t scores = 4.8 at p<0.05, FWE-corrected level respectively in the red, green and blue

1082 scale). B, D and F, this presents the receding of the stimulus respectively from near space with

1083 the small cube, from far space with the small cube or from far space with the big cube versus

1084 fixation contrast (t scores = 4.8 at p<0.05, FWE-corrected level respectively in the red, green

1085 and blue scale). On the first panel (the approach of the stimulus towards near space with the

1086 small cube), the black contours represent the near space encoding (one identified in Figure 3)

1087 and the white contours represent the specific encoding of the approach of the small cube in

1088 the near space which corresponds to the cortical regions which are activated by the approach

1089 of the small cube in the near space but not by the near space encoding (exclusive mask for the

1090 near space versus fixation baseline applied at FWE-corrected level p<0.05). For other

1091 conventions, see Figure 3.

1092

1093 **Figure 8:** Near to Far coding gradient in the arcuate sulcus (AS) and the intraparietal sulcus

1094 (IPS). A) Inflated representation of the cortex, (left and right hemisphere of the reference

48

1095    monkey cortex). The purple inset corresponds to the AS and the yellow inset corresponds to

1096    the IPS as represented in B). Black solid lines indicate the limit between the convexity and the

1097    banks of the IPS and AS; black dashed lines indicated the bottom of the sulcus. B) Prefrontal

1098    (purple inset) and parietal (yellow inset) activations of near and far space networks (group

1099    analysis superimposing the activations described in figure 4 and 5) on the same inflated maps,

1100    for the left and right hemispheres. Red to yellow color scale: selective near space coding;

1101    Red: preferential coding for near space; White: unselective coding for near and far space;

1102    Blue: preferential coding for far space; Dark blue to light blue color scale: selective near

1103    space coding. Gray regions correspond to regions activated neither by the large stimulus in far

1104    space nor by the small stimulus in near space. 5v, ventral area 5v; 7a,7b/7ab, areas 7a, 7b or

1105    7ab: MIP, medial intraparietal area MIP, V6: cortical visual area V6. For other conventions,

1106    see Figure 3, 4 and 5. Five regions of interest were defined along the AS and four along the

1107    IPS, and percentage of signal change (PSC) within each of these ROIs was extracted for each

1108    contrast of specific near space, preferential near space, unselective near and far space,

1109    preferential far space and specific far space. Below each inflated map, the PSCs are plotted

1110    for the stimulation of the small cube in the near space (orange bars) and for the stimulation of

1111    the big cube on the far space (blue bars). The specific location of each ROI as well as the map

1112    they belong to is indicated at the bottom of the figure. Statistical significance is represented as

1113    follow: *$p<0.05$; **$p<0.01$; ***$<0.001$ (paired t-tests with Bonferroni correction); o $p<0.05$

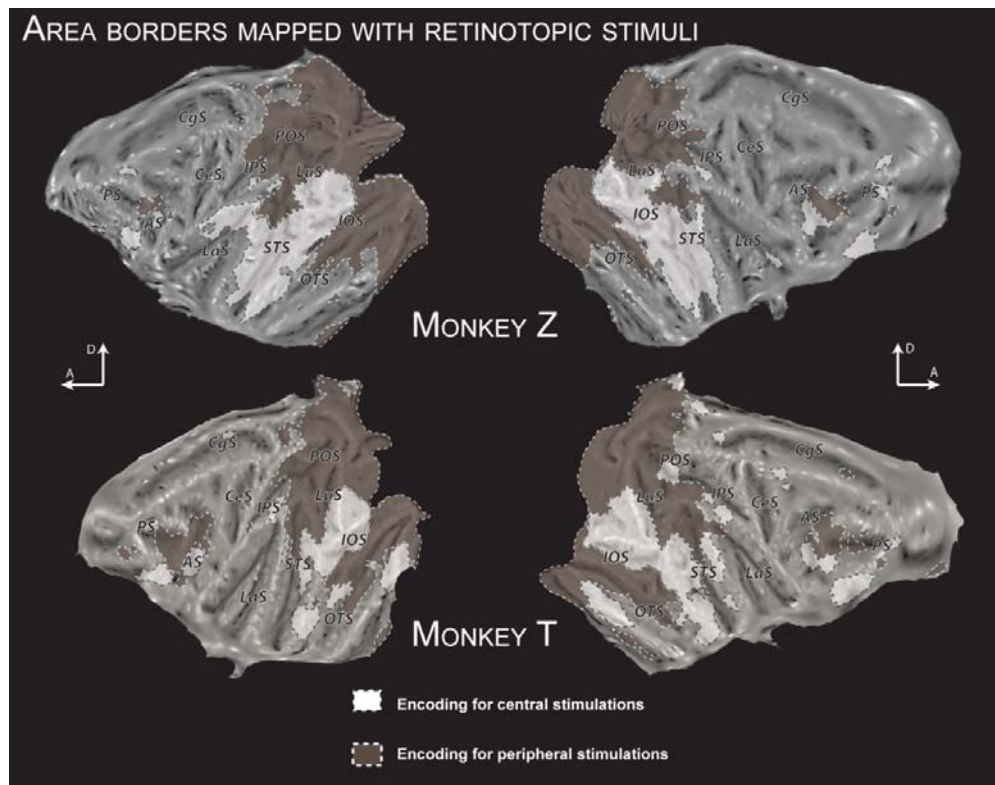1114    (paired t-tests, uncorrected).

1115

1116    **Figure S1:** Individual whole brain maps of center vs. periphery visual coding from (Guipponi

1117    et al., 2015a). Cortical sulci: AS, arcuate sulcus; CgS, cingulate sulcus; CeS, central sulcus;

1118    IOS, inferior occipital sulcus; IPS, intraparietal sulcus; LaS, lateral (Sylvian) sulcus; LuS,

1119    lunate sulcus; OTS, occipital temporal sulcus; POS, parieto-occipital sulcus; PS, principal

1120    sulcus; STS, superior temporal sulcus.
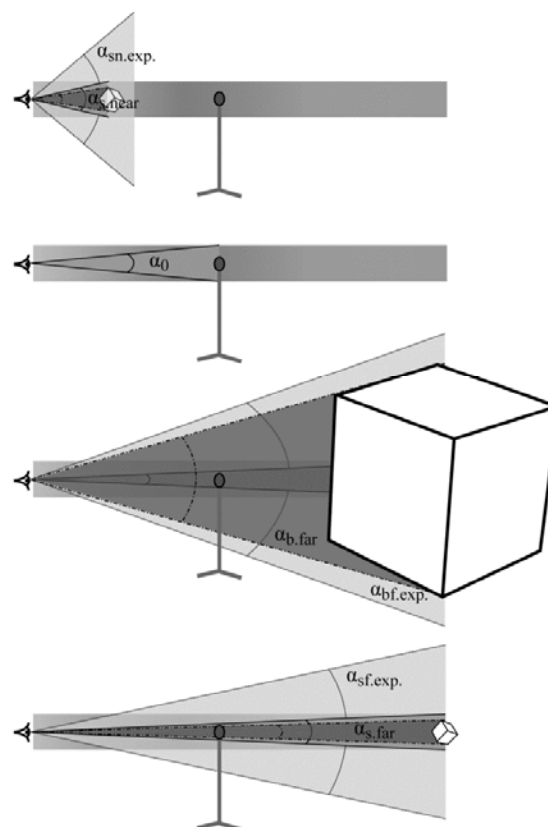
1121

1122    **Figure S2:** Graphical description of the expected range of eye movements for each type of

1123    stimuli if the monkeys had been fixating and tracking the objects rather than maintaining

1124    vergence onto the fixation spot. $\alpha_0$: angular range of eye movements when fixation is on

1125    fixation LED; $\alpha_{s.near}$: angular range of eye movements if fixation were on static small near

1126    object; $\alpha_{sn.expl}$: angular range of eye movements if fixation were on dynamic small near object

1127    (i.e. matching the experimental design); $\alpha_{b.far}$: angular range of eye movements if fixation

1128    were on static big far object; $\alpha_{bf.expl}$: angular range of eye movements if fixation were on

1129    dynamic big far object (i.e. matching the experimental design); $\alpha_{s.far}$: angular range of eye

1130    movements if fixation were on static small far object; $\alpha_{sf.expl}$: angular range of eye movements

1131    if fixation were on dynamic small far object (i.e. matching the experimental design).
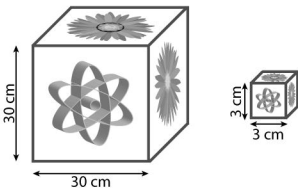
1132
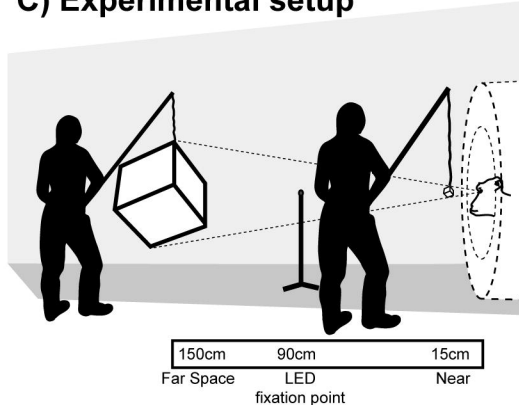
1133    **Figure S3:** Temporal signal-to-noise ratio calculated in both monkeys through the brain, in

1134    transversal view.

1135 **Supplementary data**

1136



1137

1138

1139 **Figure S1:** Individual whole brain maps of center vs. periphery visual coding from (Guipponi

1140 et al., 2015a). Cortical sulci: AS, arcuate sulcus; CgS, cingulate sulcus; CeS, central sulcus;

1141 IOS, inferior occipital sulcus; IPS, intraparietal sulcus; LaS, lateral (Sylvian) sulcus; LuS,

1142 lunate sulcus; OTS, occipital temporal sulcus; POS, parieto-occipital sulcus; PS, principal

1143 sulcus; STS, superior temporal sulcus.

1144

**Distance and width of stimulation relative to fixation point**

| Distance between stimuli and fixation point | Tolerance window width correspondance | Width of stimulation area if cube is static | Width of stimulation area if cube is moving |
|---|---|---|---|
| 15cm | 17.8° | 11.4° $\alpha_{s.near}$ | 67.4° $\alpha_{sn.expl.}$ |
| 90cm | 3° $\alpha_0$ | / | / |
| 150cm | 1.8° | 11.4° $\alpha_{b.far}$ | 15.2° $\alpha_{bf.expl.}$ |
| 150cm | 1.2° | 1.1° $\alpha_{s.far}$ | 7.6° $\alpha_{sf.expl.}$ |

**Figure S2:** Graphical description of the expected range of eye movements for each type of stimuli if the monkeys had been fixating and tracking the objects rather than maintaining vergence onto the fixation spot. $\alpha_0$: angular range of eye movements when fixation is on fixation LED; $\alpha_{s.near}$: angular range of eye movements if fixation were on static small near object; $\alpha_{sn.expl}$: angular range of eye movements if fixation were on dynamic small near object (i.e. matching the experimental design); $\alpha_{b.far}$: angular range of eye movements if fixation were on static big far object; $\alpha_{bf.expl}$: angular range of eye movements if fixation were on dynamic big far object (i.e. matching the experimental design); $\alpha_{s.far}$: angular range of eye movements if fixation were on static small far object; $\alpha_{sf.expl}$: angular range of eye movements if fixation were on dynamic small far object (i.e. matching the experimental design).
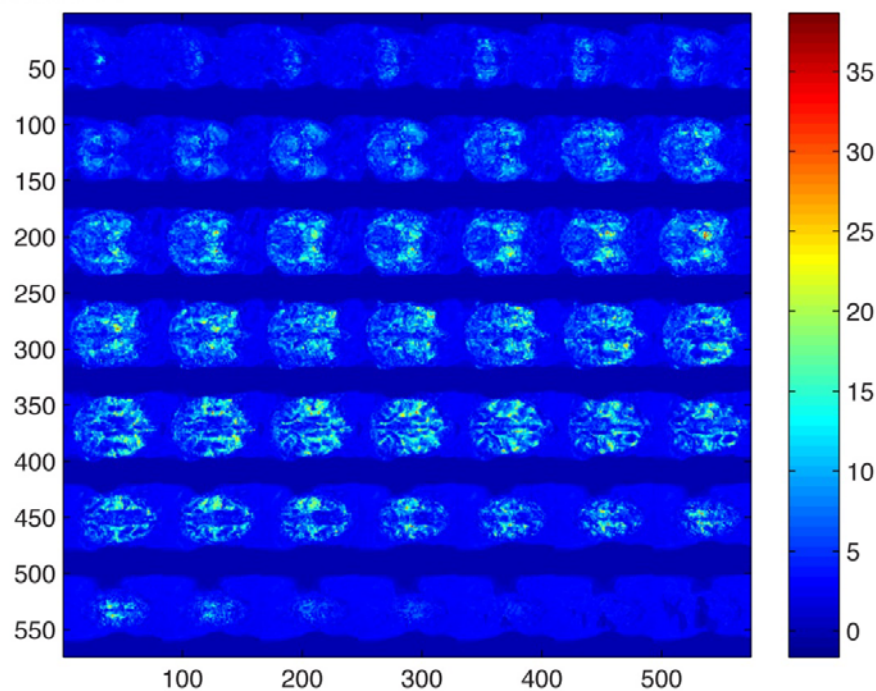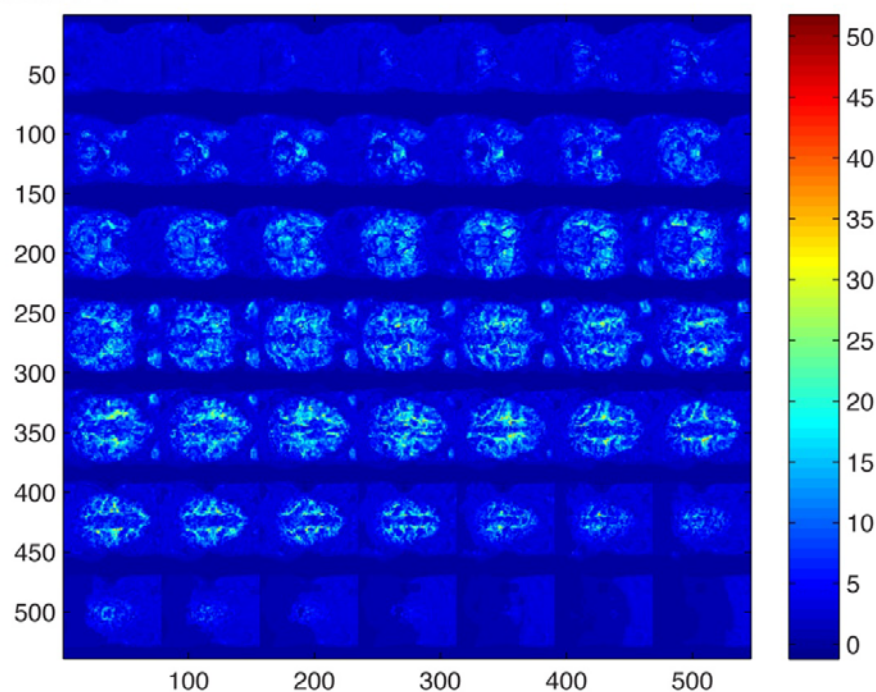
1157

**Figure S3:** Temporal signal-to-noise ratio calculated in both monkeys through the brain, in transversal view.

## A) Stimuli

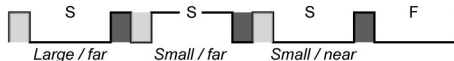30 cm × 30 cm × 30 cm

3 cm × 3 cm × 3 cm

## B) Blocked fMRI design

S   S   S   F

*Large / far*   *Small / far*   *Small / near*

S  Stimulation (13 pulses)   Cube approaching its final position (1 pulse)
F  Fixation baseline (13 pulses)   Cube withdrawal from field of view (1 pulse)

## C) Experimental setup

| 150cm | 90cm | 15cm |
|---|---|---|
| Far Space | LED fixation point | Near |

## D) Summary of the contrast analyses

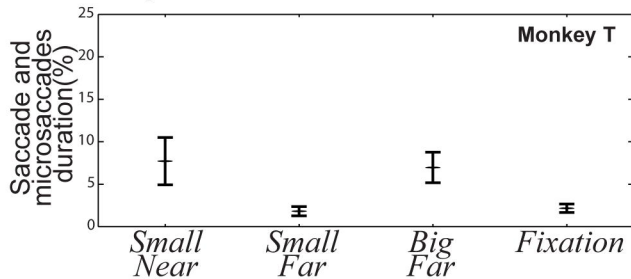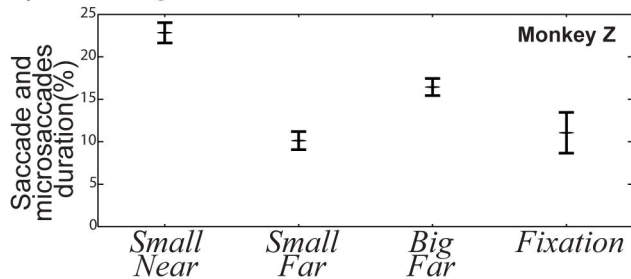| Small Near space | Preferential Near space | Selective Near space |
|---|---|---|
| Small Near >> Fixation | Small Near >> Big Far **AND** Small Near >> Fixation *(inclusive mask)* **(1)** | Small Near >> Big Far **AND** Small Near >> Fixation *(inclusive mask)* **AND** NOT Big Far >> Fixation *(exclusive mask)* **(2)** |
| Big Far space | Preferential Far space | Selective Far space |
| Big Far >> Fixation | Big Far >> Small Near **AND** Big Far >> Fixation *(inclusive mask)* **(3)** | Big Far >> Small Near **AND** Big Far >> Fixation *(inclusive mask)* **AND** NOT Small Near >> Fixation *(exclusive mask)* **(4)** |
| Small Far space | Preferential Object size | Selective Object size |
| Small Far >> Fixation | Big Far >> Small Far **AND** Big Far >> Fixation *(inclusive mask)* **(4)** | Big Far >> Small Far **AND** Big Far >> Fixation *(inclusive mask)* **AND** NOT Small Far >> Fixation *(exclusive mask)* **(6)** |
| Looming Near object | Preferential Looming | Selective Looming |
| Looming >> Fixation | Looming >> Small Near **AND** Looming >> Fixation *(inclusive mask)* **(5)** | Looming >> Small Near **AND** Looming >> Fixation *(inclusive mask)* **AND** NOT Small Near >> Fixation *(exclusive mask)* **(8)** |

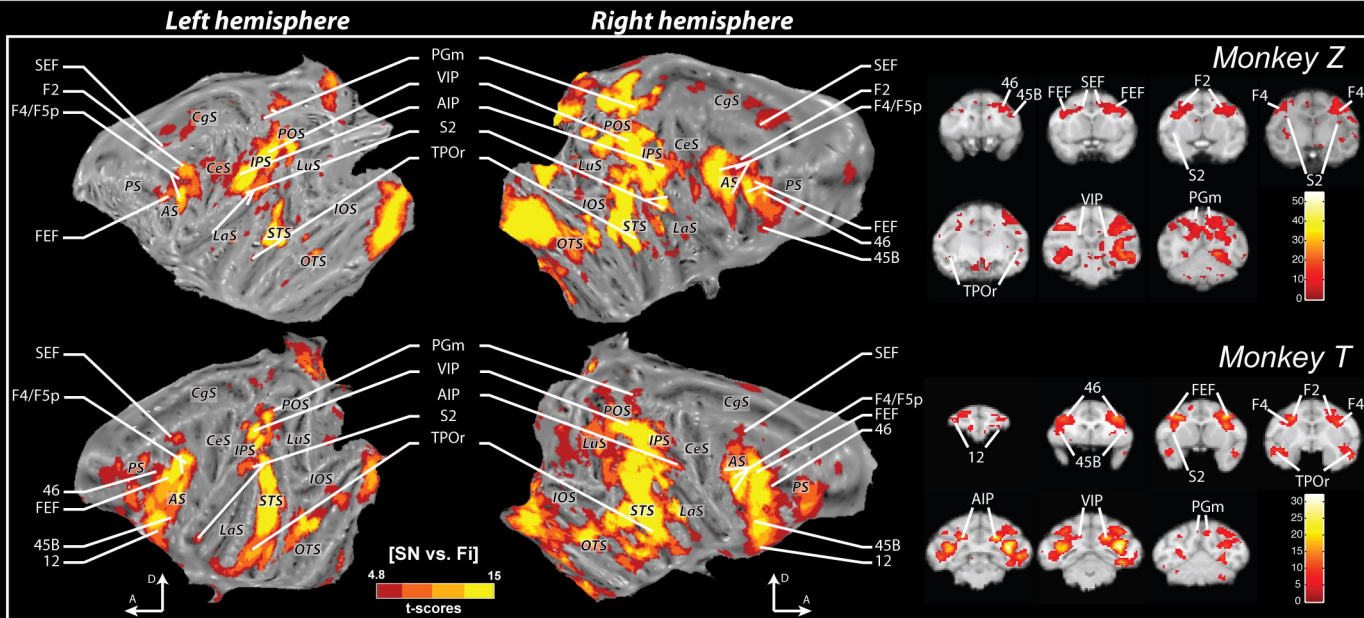**A) Example of a run for X eye position trace**
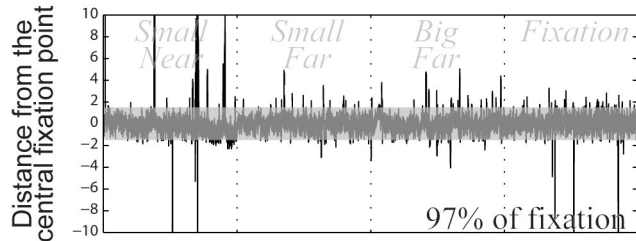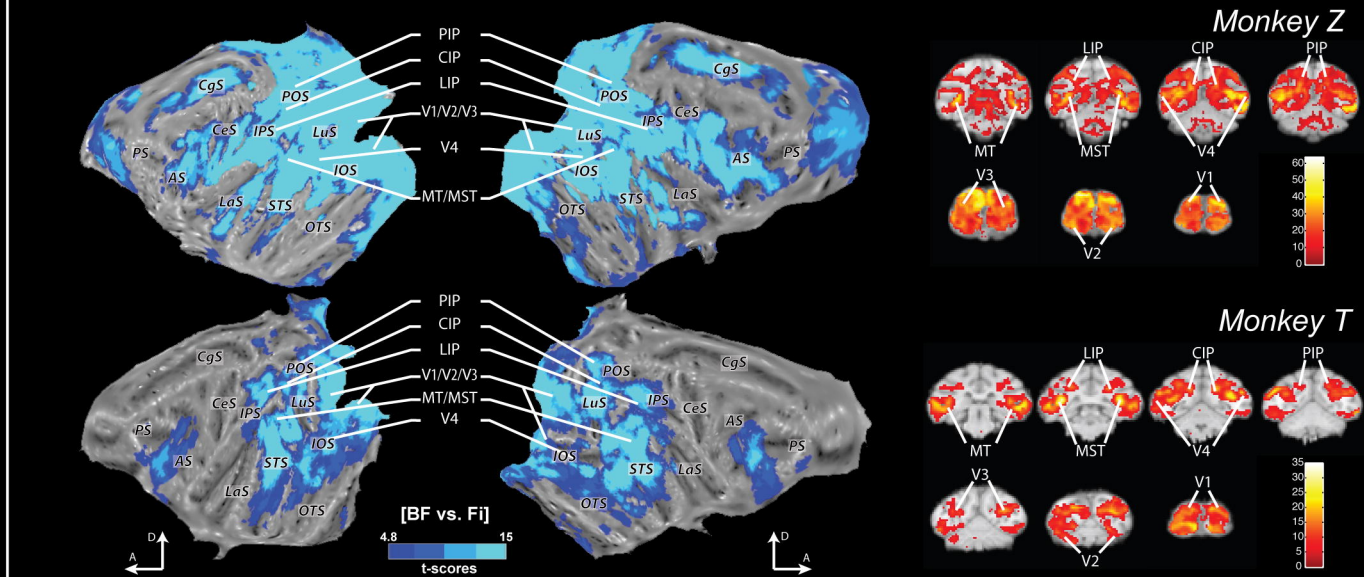


**B) Example of a run for Y eye position trace**
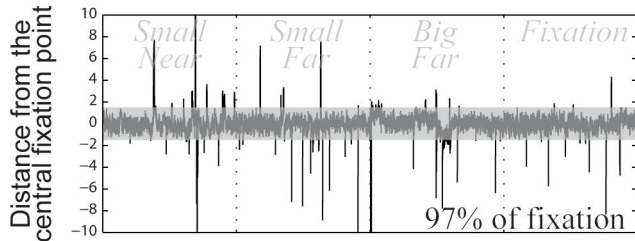


**C) Percentage of saccades and microsaccades duration with respect to the total block duration in both monkeys**
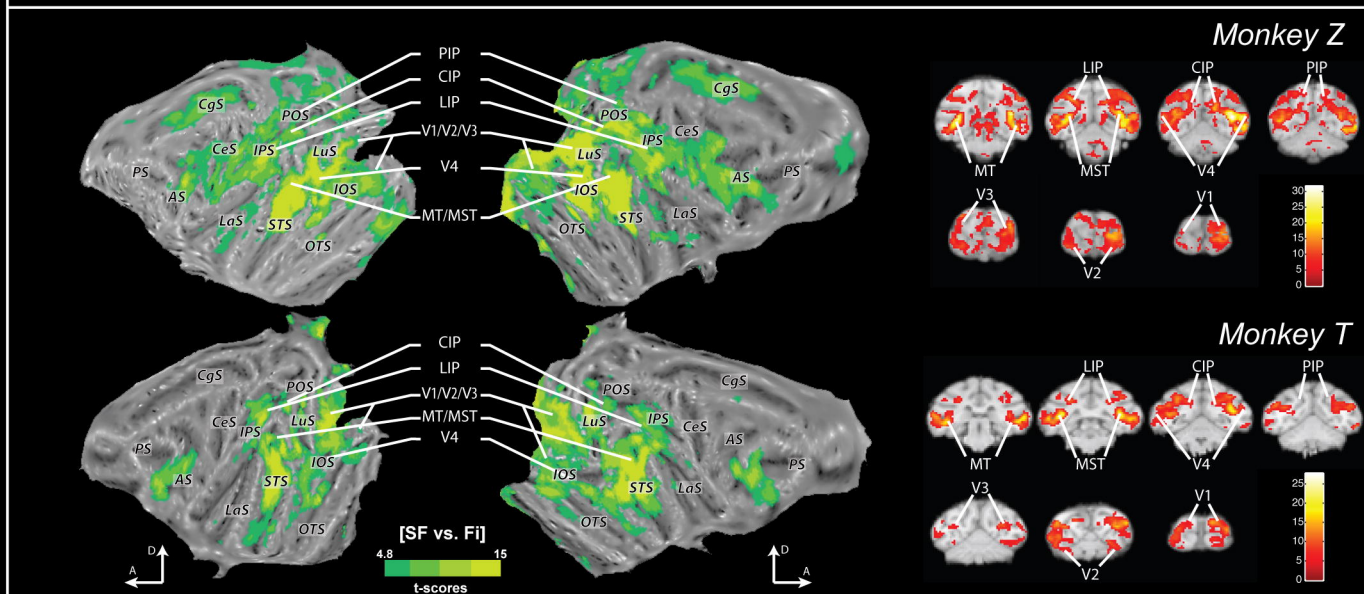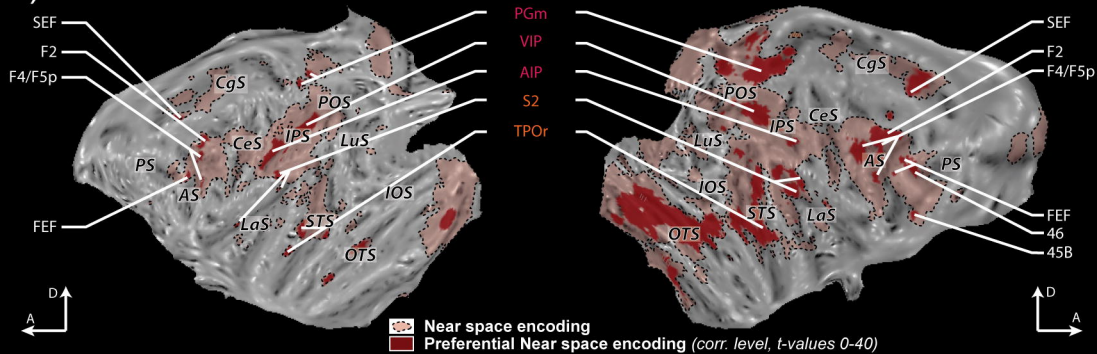
**Dorsal parieto-frontal network** / **Ventral temporo-frontal network**
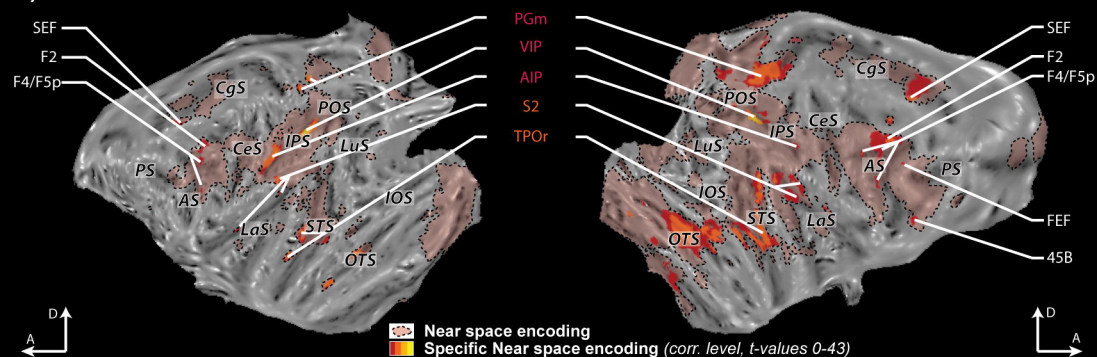
**A) PREFERENTIAL NEAR SPACE ENCODING IN MONKEY Z**

Near space encoding
Preferential Near space encoding (corr. level, t-values 0-40)

**B) SELECTIVE NEAR SPACE ENCODING IN MONKEY Z**

Near space encoding
Specific Near space encoding (corr. level, t-values 0-43)

**C) PREFERENTIAL NEAR SPACE ENCODING IN MONKEY T**

Near space encoding
Preferential Near space encoding (corr. level, t-values 0-13.1)

**D) SELECTIVE NEAR SPACE ENCODING IN MONKEY T**

Near space encoding
Specific Near space encoding (corr. level, t-values 0-11)

**Striate and extrastriate visual cortex** / **Parietal and dorso-temporal regions**
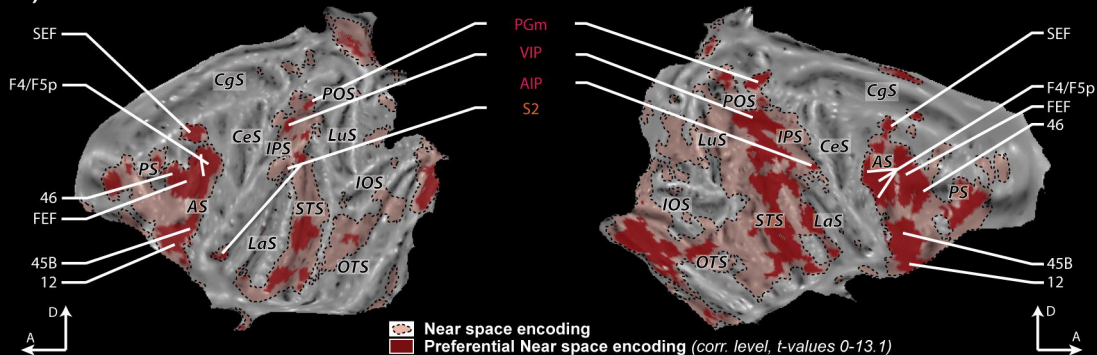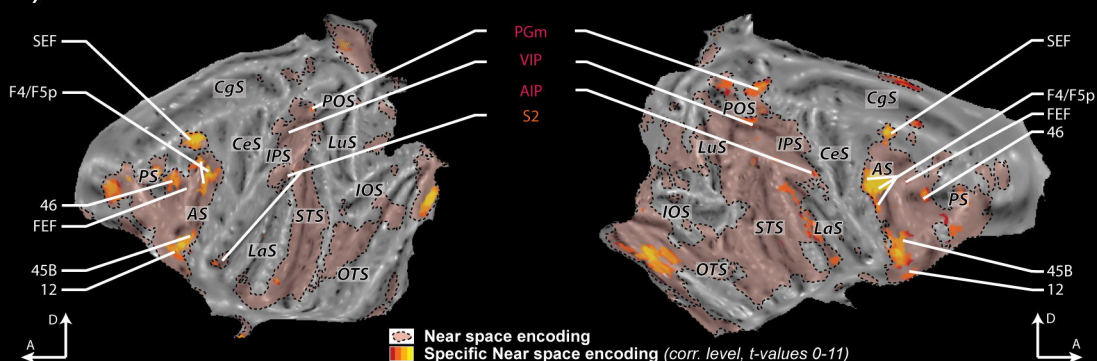
A) PREFERENTIAL FAR SPACE ENCODING MONKEY Z
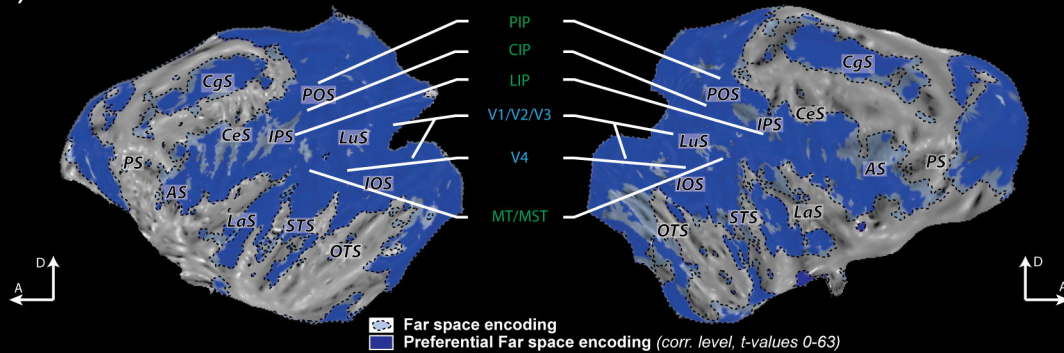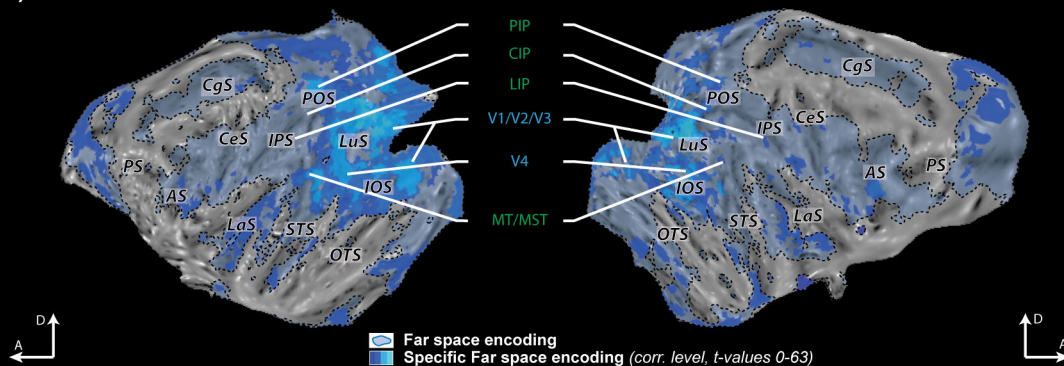
Far space encoding
Preferential Far space encoding (corr. level, t-values 0-63)

B) SELECTIVE FAR SPACE ENCODING IN MONKEY Z

Far space encoding
Specific Far space encoding (corr. level, t-values 0-63)

C) PREFERENTIAL FAR SPACE ENCODING IN MONKEY T

Far space encoding
Preferential Far space encoding (corr. level, t-values 0-19.3)

D) SELECTIVE FAR SPACE ENCODING IN MONKEY T

Far space encoding
Specific Far space encoding (corr. level, t-values 0.21.7)

*Group analysis*

**Left** **Right**

CgS

POS

CeS IPS LuS

AS

PS

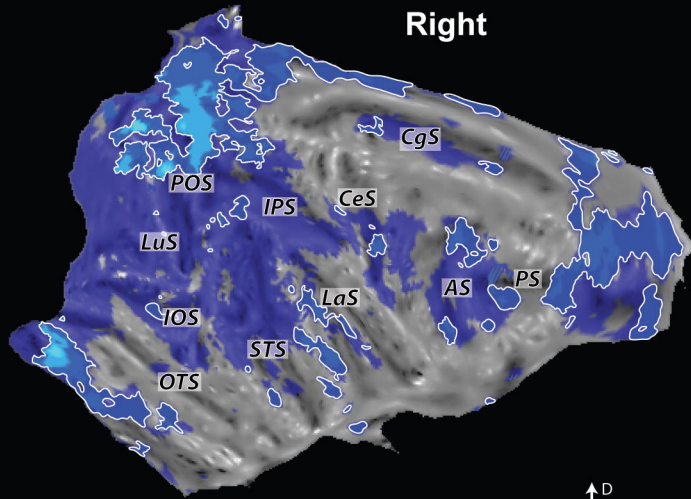LaS IOS

STS OTS

CgS

POS IPS CeS
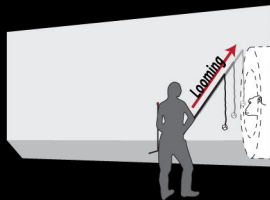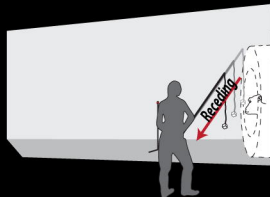
LuS

AS PS

LaS

IOS STS

OTS

D

A

D

A
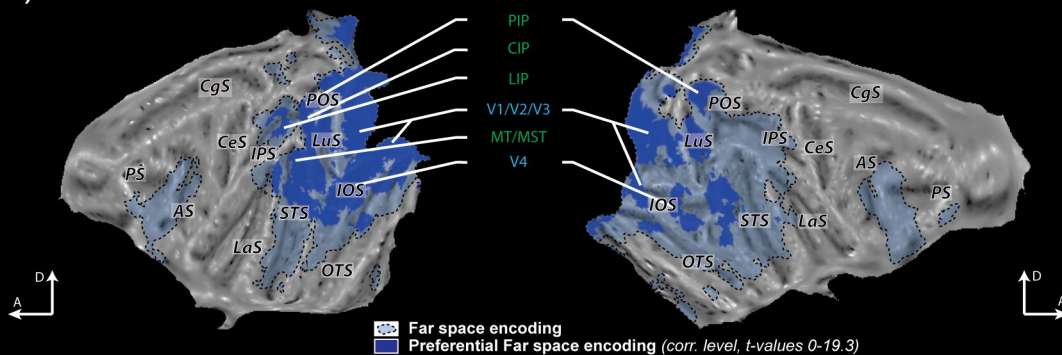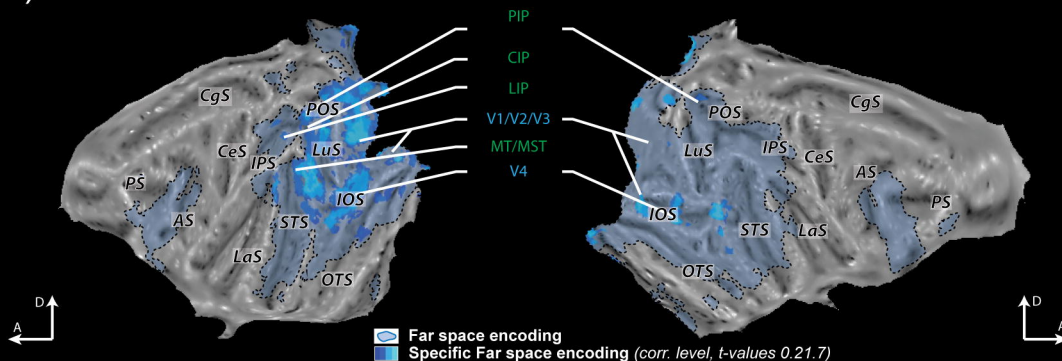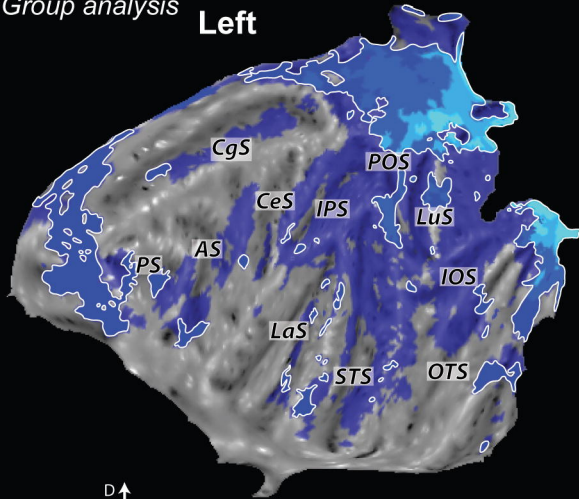
■ **Specific encoding of the large cube in the far space** *(corrected level)*
■ **Preferential encoding of the large cube in far space**

A) Small cube Looming towards Near space

B) Small cube Receding from Near space

C) Small cube Looming towards Far space
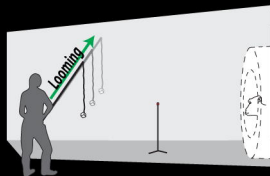
D) Small cube Receding from Far space
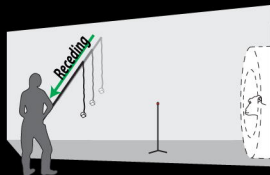
E) Big cube Looming towards Far space

F) Big cube Receding from Far space

Group analysis

Looming
Receding

CgS  POS  IPS  LuS  CeS  PS  AS  STS  IOS  LaS  OTS

t-scores 4.8 — 10

Specific looming towards near space encoding (corrected level)
Near space encoding (t-scores 4.8-10)

t-scores 4.8 — 10

Specific looming towards far space encoding (corrected level)

t-scores 4.8 — 10

Specific looming towards far space encoding (corrected level)

**A) INFLATED MAPS**

*Left hemisphere*

*Right hemisphere*

**B) FOCUS ON PREFRONTAL AND PARIETAL CORTEX**

*Group analysis*

*Left prefrontal cortex*

*Left parietal cortex*

*Right prefrontal cortex*

*Right parietal cortex*

**Near ↕ Far**

- Specific Near space encoding *(corrected level)*
- Preferential Near space encoding *(corrected level)*
- Unselective Near and Far space encoding *(corrected level)*
- Preferential Far space encoding *(corrected level)*
- Specific Far space encoding *(corrected level)*

**Left prefrontal cortex**

**Left parietal cortex**

■ Small near stimulation  ■ Big far stimulation

ROI 1 [-7;2;17]  ROI 2 [-9;0;12]  ROI 3 [-13;-3;9]  ROI 4 [-16;-3;9]  ROI 5 [-19;1;11]  ROI 6 [-13;-15;11]  ROI 7 [-10;-17;9]  ROI 8 [-10;-28;13]  ROI 9 [-10;-28;2]

**Right prefrontal cortex**

**Right parietal cortex**

ROI 1 [4;2;17]  ROI 2 [14;-2;8]  ROI 3 [13;0;9]  ROI 4 [14;2;7]  ROI 5 [14;5;6]  ROI 6 [6;-21;4]  ROI 7 [12;-23;13]  ROI 8 [15;-21;13]  ROI 9 [18;-17;13]